HHS Public Access

Author manuscript

*Cell Calcium*. Author manuscript; available in PMC 2016 November 01.

Published in final edited form as:

*Cell Calcium*. 2015 November ; 58(5): 476–488. doi:10.1016/j.ceca.2015.07.004.

# Effect of M-phase kinase phosphorylations on type 1 inositol 1,4,5-trisphosphate receptor-mediated $Ca^{2+}$ responses in mouse eggs

**Nan Zhang**[1,2], **Sook Young Yoon**[3], **Jan B. Parys**[4], and **Rafael. A. Fissore**[1,*]

[1]Department of Veterinary and Animal Sciences, University of Massachusetts, Amherst, MA 01003, USA

[2]Department of Obstetrics and Gynecology, Feinberg School of Medicine, Northwestern University, Chicago, IL 60611, USA

[3]Fertility Center of CHA Gangnam Medical Center, College of Medicine, CHA, University, Seoul 135-081, Korea

[4]KU Leuven, Laboratory of Molecular and Cellular Signaling, Department of Cellular and Molecular Medicine, Campus Gasthuisberg O/N-I box 802, Herestraat 49, BE-3000 Leuven, Belgium

## Abstract

The type 1 inositol 1,4,5-trisphosphate receptor ($IP_3R1$) mediates increases in the intracellular concentration of $Ca^{2+}$ ($[Ca^{2+}]_i$) during fertilization in mammalian eggs. The activity of $IP_3R1$ is enhanced during oocyte maturation, and phosphorylations by M-phase kinases are thought to positively regulate the activity of $IP_3R1$. Accordingly, we and others have found that $IP_3R1$ is phosphorylated at $S^{421}$, $T^{799}$ (by Cdk1) and at $S^{436}$ (by ERK). Nevertheless, the effects of these phosphorylations on the function of the receptor and their impact on $[Ca^{2+}]_i$ oscillations in eggs have not been clearly examined. To address this, we expressed in mouse oocytes an $IP_3R1$ variant with the three indicated phosphorylation sites replaced by acidic residues, IIIE-$IP_3R1$, such that it would act like a constitutively phosphorylated $IP_3R1$, and examined $[Ca^{2+}]_i$ parameters in response to stimuli. We found that overexpression of wild type (wt-$IP_3R1$) or IIIE-$IP_3R1$ in oocytes containing endogenous receptors caused dominant negative-like effects on $Ca^{2+}$ release and oscillations. Therefore, we first selectively removed the endogenous $IP_3R1$, and subsequently expressed the exogenous receptors. We found that in response to injection of PLCζ cRNA, eggs without endogenous $IP_3R1$ failed to mount persistent $Ca^{2+}$ oscillations, although expression of wt-$IP_3R1$ restored their $[Ca^{2+}]_i$ oscillatory activity. We also observed that the $Ca^{2+}$ oscillatory ability and the sensitivity to $IP_3$ in eggs expressing IIIE-$IP_3R1$ were greater than in those expressing wt-$IP_3R1$. Lastly, we found that exogenous $IP_3R1$s are resistant to downregulation and support longer

[*]**Address for Correspondence**: Department of Veterinary and Animal Sciences, ISB-661 North Pleasant Street, University of Massachusetts Amherst, Massachusetts 01003, USA. Tel: (413) 545-5548; Fax: (413) 545-6326; rfissore@vasci.umass.edu.

oscillations and of higher amplitude. Altogether, our results show that phosphorylations by Cdk1 and MAPK enhance the activity of $IP_3R1$, which is consistent with its maximal activity observed at the time of fertilization and the role of $Ca^{2+}$ release in egg activation.

## Graphical Abstract

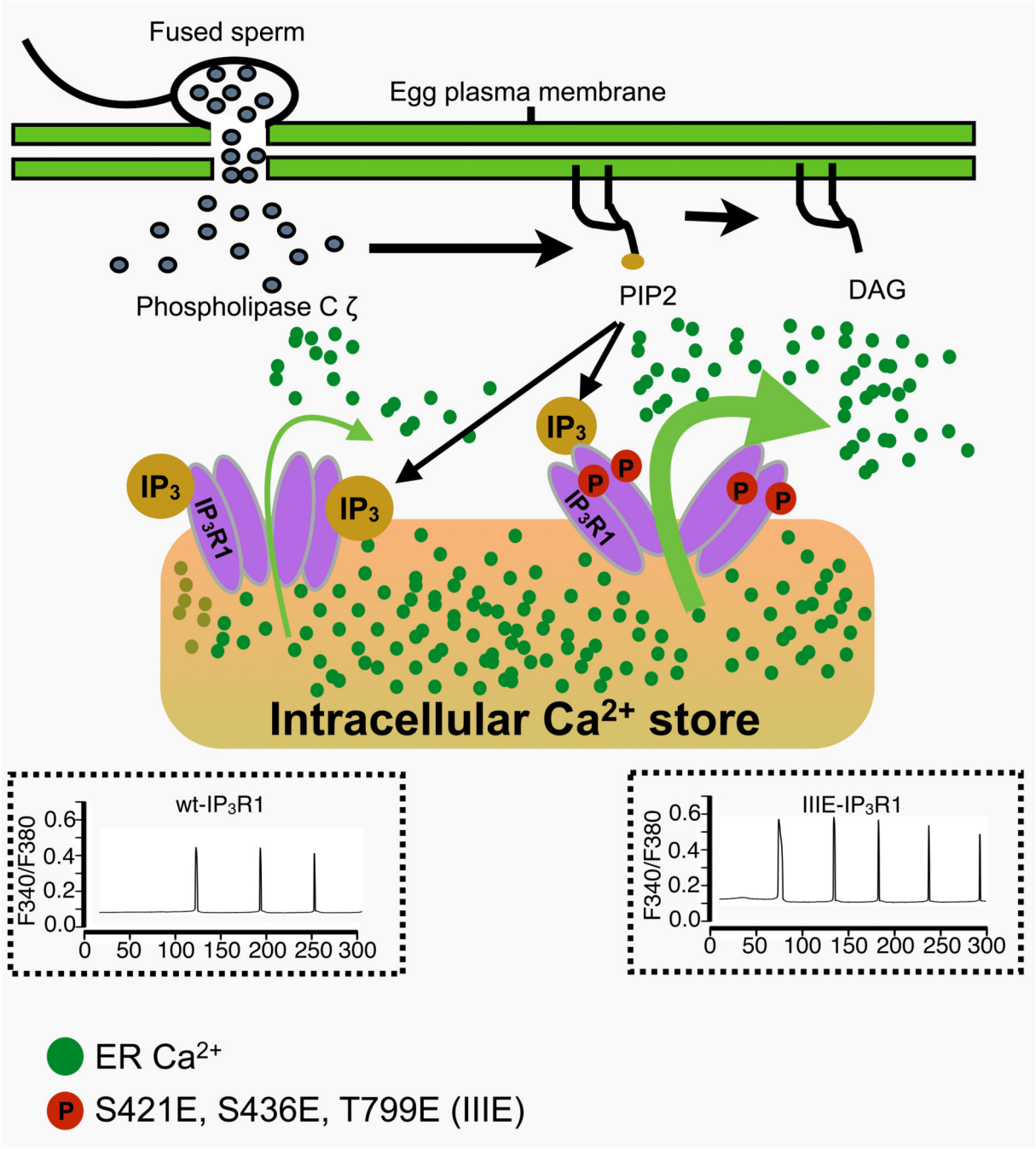

## INTRODUCTION

In preparation for fertilization, ovulated mammalian eggs are arrested at the metaphase stage of the second meiotic division (MII). Fertilization initiates a series of signaling and cellular events that result in the release of cortical granules (CG), block to polyspermy, resumption and completion of meiosis, pronuclear (PN) formation and progression into interphase followed by the first mitosis. These events collectively make possible the transition from meiotic into mitotic/embryonic stages and are collectively referred to as “egg activation” [1–3]. In all species studied to date, an increase in the intracellular concentration of free calcium ($[Ca^{2+}]_i$) underlies egg activation [2, 4, 5]. In mammals, $[Ca^{2+}]_i$ rises occur periodically and are referred to as $[Ca^{2+}]_i$ oscillations [2, 6–8]. A testis-specific phospholipase C (PLC), PLCζ [9], which is thought to be delivered into the ooplasm after fusion of the gametes, hydrolyzes phosphatidylinositol 4,5-bisphosphate ($PIP_2$) and produces inositol 1,4,5-trisphosphate ($IP_3$). The latter is the ligand for the $IP_3$ receptor ($IP_3R$), a tetrameric intracellular $Ca^{2+}$ channel whose isoform 1 ($IP_3R1$) is most abundant in eggs and mediates most of the $Ca^{2+}$ release during mammalian fertilization [10–12]; $IP_3R1$ is predominantly located in the endoplasmic reticulum (ER), the eggs’ main $Ca^{2+}$ reservoir [13, 14].

Each $IP_3R1$ monomer is composed of over 2700 amino acids and forms a large protein of ~300 kDa [15, 16]. It can be divided into three main domains: a cytosolic N-terminal ligand-binding domain, a middle regulatory domain that contains binding sites for numerous regulatory molecules including $Ca^{2+}$, ATP and modulatory proteins [17–19], and a C-terminal domain consisting of six transmembrane segments that terminate in a short tail that extends into the ooplasm [16]. The two main agonists of $IP_3R1$ are $IP_3$ and $Ca^{2+}$. The $Ca^{2+}$ release mediated by these agonists adopts a bell-shape dose-response with respect to $Ca^{2+}$ concentrations, as the activity of $IP_3R1$ is enhanced at intermediate $[Ca^{2+}]_i$ and inhibited at high or low $[Ca^{2+}]_i$ extremes [20–23]. This close regulation of $IP_3R1$ by $Ca^{2+}$ makes possible the repeated and episodic $Ca^{2+}$ release that underlies the generation of long lasting oscillations.

Vertebrate eggs acquire the ability to support the precise spatiotemporal pattern of fertilization-associated $[Ca^{2+}]_i$ oscillations during oocyte maturation [24, 25]. During this process, the receptor’s ability to release $Ca^{2+}$, here defined as $IP_3R1$ sensitivity, is gradually enhanced [24, 26, 27]. This enhancement is thought to be due to the changes in $IP_3$ binding affinity and/or enhanced open probability of the receptor [21, 22, 26]. Although it has been investigated for many years, the molecular mechanism(s) underlying the exquisite modulation of $IP_3R1$’s function is still unresolved [17, 28, 29]. Phosphorylation is a major signaling mechanism involved in regulating the function of $IP_3R1$ in many cell systems [17, 30, 31]. Sequence analysis has shown that $IP_3R1$ possesses phosphorylation consensus sites for many kinases, although the functional impact of these modifications has not been completely examined [15, 17]. In mouse oocytes, $IP_3R1$ becomes progressively phosphorylated during maturation at an MPM-2 epitope, which is phosphorylated by one of several mitosis-associated kinases [32], and this coincides with enhanced receptor function at the MII stage, the stage of fertilization [33]. After fertilization, $IP_3R1$ undergoes gradual dephosphorylation, which concurs with reduced $Ca^{2+}$ release during this period [33, 34].

These data suggest that cell cycle-associated phosphorylations most likely by M-phase kinases regulate the function of $IP_3R1$ in eggs.

Two canonical M-phase kinases, Cdk1 and MAPK/ERK, are known to phosphorylate either Ser/Thr residues preceding a Pro residue; hence the denomination of Proline (P) targeted kinases. These kinases are responsible for the resumption and progression of meiosis during maturation [35]. Sequence analysis of $IP_3R1$ has revealed conserved kinase motifs, including three Cdk1 consensus sites, $S^{421}PVK$, $T^{799}PVK$ and $S^{2147}PR$ [36] and an ERK site, $PVS^{436}P$ [37]. Studies in DT40 cells using *in vitro* kinase assays demonstrated $IP_3R1$ phosphorylation at $S^{421}$ and $T^{799}$ [38] and these residues were also found to be phosphorylated in *in vitro* maturated mouse oocytes by site-specific antibodies [28]. Phosphorylation at the $S^{436}$ site by ERK was confirmed by in *vivo and in vitro* studies using somatic cells and mouse eggs [33, 39]. Despite this evidence, the impact of these phosphorylations on receptor function and oscillations has not been resolved. For example, while it was reported that phosphorylation at $S^{436}$ suppressed $Ca^{2+}$ release in ER microsomes from somatic cells [39, 40], inhibition of MAPK kinase reduced MPM-2 phosphorylation and $[Ca^{2+}]_i$ oscillations in mouse eggs [33]. Nevertheless, in the latter study, the pharmacological inhibitor U0126 was used to prevent MAPK activation, which was later shown to alter $Ca^{2+}$ homeostasis in other unpredictable ways [7, 41].

To more carefully examine the role of phosphorylation on $IP_3R1$ function, we developed an *in vivo* system in which endogenous $IP_3R1$ protein is selectively knocked down ($IP_3R1$-KD eggs) and this is followed by expression of exogenous wildtype (wt) or modified versions of mouse $IP_3R1$ (IIIE-$IP_3R1$). $[Ca^{2+}]_i$ oscillations induced by injection of PLCζ cRNA were then monitored to ascertain the effect of $IP_3R1$ modifications. We found that expression of exogenous wt-$IP_3R1$ in $IP_3R1$-KD eggs restored the ability of these eggs to support long-lasting $[Ca^{2+}]_i$ oscillations, although with lower sensitivity and periodicity than those displayed by control eggs. Expression of $IP_3R1$ with phosphomimetic mutations supported significantly higher functional activity than the wt-$IP_3R1$, demonstrating for the first time the role of phosphorylation and M-phase kinases in regulating $IP_3R1$ function in mouse oocytes and eggs.

## RESULTS

### Expression of exogenous $IP_3R1$ in mouse eggs and its effects on $[Ca^{2+}]_i$ oscillations

The fundamental role of $IP_3R1$ on mammalian fertilization is well established [12], although how it is regulated during maturation and fertilization remains to be resolved. Phosphorylation is a mechanism thought to influence $IP_3R1$ function in this process [33, 38–40, 42], although *in vivo* studies using expression of mutant receptors in mammalian oocytes and eggs have not yet been performed. Therefore, to investigate the impact of phosphorylation on $IP_3R1$ channel activity, we generated a wild type construct and one encoding for phosphomimetic mutations at the two Cdk1 sites and at the one ERK site (wt-$IP_3R1$ and IIIE-$IP_3R1$ in Fig. 1A), as all these sites have been shown to affect receptor function in somatic cells and *in vitro* studies [38, 39, 42]. Therefore, $S^{421}$ and $T^{799}$ within Cdk1 sites, and $S^{436}$, within the ERK motif, were replaced with aspartic acid. For expression and functional studies, these constructs were tagged with 6xHis.

All constructs were *in vitro* transcribed into cRNAs, which were then injected into GV oocytes, as described in Materials and Methods. Protein expression of exogenous receptors was confirmed in GV oocytes collected at 4–6 hr after cRNAs injection (Fig. 1B). Control oocytes injected with microinjection buffer (MIB) showed at ~270 kDa the signal corresponding to the endogenous $IP_3R1$ (Fig. 1B; MIB). In oocytes injected with either of the constructs (Fig. 1B; wt-$IP_3R1$ and IIIE-$IP_3R1$), the signal corresponding to $IP_3R1$ was greatly enhanced suggesting that some of the exogenous receptor was running together with the endogenous protein. In addition, in eggs expressing exogenous proteins, an additional, faint band that run above the endogenous receptors was observed, suggesting that 6xHis tag might slow the migration of $IP_3R1$.

Having demonstrated the expression of exogenous $IP_3R1$ receptors in mouse eggs, we subsequently analyzed how their expression impacted $[Ca^{2+}]_i$ responses induced by injection of 0.05 μg/μl of PLCζ cRNA, which was used as a proxy for fertilization. GV oocytes were injected with $IP_3R1$s cRNAs or ER-DsRed cRNA and matured for 12–14 hr, after which eggs that had extruded the 1st polar body were selected for $Ca^{2+}$ monitoring. ER-DsRed cRNA, which encodes for a red fluorescent protein with an ER targeting signal, was used as an additional control for expression of an ER-targeted protein. Injection of MIB or expression of ER-DsRed cRNA did not alter the normal pattern of $[Ca^{2+}]_i$ responses induced by PLCζ expression, which characteristically started ~50 min post injection and lasted for ~180 min (Fig. 1C, D). Surprisingly, expression of exogenous $IP_3R1$s proteins greatly delayed the initiation of $[Ca^{2+}]_i$ responses after injection, although expression of wt-$IP_3R1$ was more detrimental than that caused by expression of IIIE-$IP_3R1$, 78.9±22.4 and 68.5±15.9 min, respectively (Fig. 1D, $P<0.05$). Eggs expressing exogenous $IP_3R1$s also mounted oscillations of reduced frequency and amplitude compared to controls (Fig. 1C, E and F). Collectively, the data show that the expression of exogenous $IP_3R1$s compromises the function of endogenous $IP_3R1$s causing dominant negative-like effects. Therefore, under these conditions, it was not possible to examine the effect of phosphorylation on the function of $IP_3R1$ in mouse eggs.

## Expression of wt-$IP_3R1$ in mouse eggs with ligand-induced $IP_3R1$ knockdown ($IP_3R1$-KD)

Given the limitation of the previous approach, we developed an *in vivo* system in which endogenous $IP_3R1$s were first selectively downregulated by Adenophostin A (AdA), a non-hydrolyzable agonist of $IP_3R1$ that induces rapid and almost complete degradation of $IP_3R1$ [34, 43]. The cRNAs encoding for the selected exogenous receptors were subsequently injected 4 hours after AdA injection and the oocytes were further *in vitro* matured for 14 hr. After this period, eggs with 1st polar bodies were selected to examine $IP_3R1$ and ER distribution and to confirm levels of protein expression. Injection of AdA caused degradation of most of the endogenous $IP_3R1$ (Fig. 2A, upper panel, 3rd lane from left; +AdA – wt-IP3R1 cRNA), while injection of wt-$IP_3R1$ cRNA returned expression of $IP_3R1$ to levels similar to those observed prior to downregulation (Fig. 2A, upper panel, 2nd lane from left; +AdA +wt-$IP_3R1$). As expected, control eggs injected with MIB maintained $IP_3R1$ expression (Fig. 2A, upper panel 1st lane from left; -AdA -wt-$IP_3R1$). Confirmation of expression of exogenous receptors was demonstrated by western blotting using an α-His antibody (Fig. 2A, lower panel, middle lane).

We first examined the ER organization as well as the distribution of $IP_3R1$ in $IP_3R1$-KD eggs expressing wt-$IP_3R1$. We used a variety of methods to evaluate the distribution of the ER, including the ER marker $DiIC_{18}$, which is a lipophilic dicarbocyanine dye [44, 45], and the more specific ER marker, ER-DsRed cRNA, and this was done with the expectation that their different technical requirements (Materials and Methods) and particular advantages may provide a more thorough evaluation of the status of the ER following knockdown of $IP_3R1$s. For $DiIC_{18}$ imaging, examination under confocal microscopy was performed 30 to 60 min post-injection of soybean oil saturated with $DiIC_{18}$; in our hands the cortical clusters revealed by this procedure were somewhat less distinct than previously reported [46] and we attribute this discrepancy to the fact our images were captured using *in vitro* matured eggs, which are known to display less conspicuous cortical clusters than *in vivo* matured eggs [46, 47]. We found that whereas the absence of endogenous $IP_3R1$ receptors left the overall distribution of the ER mostly unaffected, the stereotypical cortical clusters and cortical enrichment were largely absent in $IP_3R1$-KD eggs (Fig. 2B–h). Expression of wt-$IP_3R1$ in $IP_3R1$-KD did not affect the organization of the ER and did not increase the presence of cortical ER clusters, as revealed by this method (Fig. 2B–i). It is worth noting that on occasions we observed large patches of fluorescence, which we estimated represented non-specific accumulation of $DiIC_{18}$ (Fig. 2B–g,i and inset), as they were not seen with other methods (see below). To confirm the distribution of the ER in $IP_3R1$-KD eggs expressing wt-$IP_3R1$, we also used ER-DsRed cRNA injection in the various conditions. When assessed with this technique, the ER was homogeneously distributed in all groups (Fig. 2B–a,b,c and insets), although the reduced presence of cortical clusters caused by $IP_3R1$-KD was not rescued by expression of wt-$IP_3R1$ (Fig. 2B–c; insets). In spite of this, the presence of cortical ER in both KD and KD+wt-$IP_3R1$ eggs was greater with this method than with $DiIC_{18}$. Quantification of clusters ≥1 μm in diameter in these ER-DsRed cRNA injected eggs revealed ~30% less clusters in KD and KD+wt-$IP_3R1$ eggs than in control eggs (Fig. 2C; $P<0.05$). Lastly, we used transmission electron microscopy (TEM) to evaluate the ER ultrastructure of these eggs. As previously reported by others [45], GV oocytes displayed very few clusters of vesicular smooth ER (SER) near the plasma membrane (Fig. 2D–a), although eggs accumulated SER vesicles near the plasma membrane (Fig. 2D–b), which are the “so called” cortical clusters observed with less discerning microscopy methods. Importantly, $IP_3R1$-KD eggs exhibited reduced presence of SER clusters (Fig. 2D–c), which was not rescued by expression of wt-$IP_3R$ (Fig. 2D–d).

We next examined the distribution of wt-$IP_3R1$ in $IP_3R1$-KD eggs. For these studies it was necessary to perform immunofluorescence, as the fluorescent signal generated by expression of Venus tagged wt-$IP_3R1$ in live MII eggs was too weak to be detected by confocal microscopy [48]. As expected, in control eggs, endogenous $IP_3R1$ was present throughout the ooplasm corresponding to the distribution of the ER, including the formation of conspicuous cortical clusters (Fig. 2B–d; arrowheads and insets). In $IP_3R1$-KD eggs the $IP_3R1$ signal was virtually undetectable (Fig. 2B–e), while expression of wt-$IP_3R1$ re-established the $IP_3R1$ signal and the receptors showed a similar distribution to that of endogenous receptors, including enhanced cortical location (Fig. 2B–f). Collectively, our results show that our method of $IP_3R1$-KD does not interfere with the pattern of ER reorganization during maturation, except that formation of cortical clusters is reduced.

Further, injection of wt-$IP_3R1$ cRNA rescued $IP_3R1$ mass and distribution in $IP_3R1$-KD eggs, although it did not restore ER cortical organization, suggesting that exogenous wt-$IP_3R1$s in oocytes and eggs do not undergo the same modifications than endogenous receptors and/or fail to associate with appropriate partner proteins. Further, these results seem to imply that $IP_3R1$s alone are not sufficient to drive the formation of ER cortical clusters in mouse eggs.

## Expression of exogenous $IP_3R1$s in $IP_3R1$-KD eggs and the ER releasable $Ca^{2+}$ pool

Prior to examining the capacity of exogenous $IP_3R1$s to support $Ca^{2+}$ oscillations, we investigated whether or not the ER releasable $Ca^{2+}$ content ($[Ca^{2+}]_{ER}$) was disturbed by $IP_3R1$-KD, as $[Ca^{2+}]_{ER}$ is thought to influence $IP_3R1$ sensitivity [49–52]. Several standard methods were used to test this parameter, including ionomycin (Iono), which when added to cells maintained in medium devoid of extracellular $Ca^{2+}$ promotes $Ca^{2+}$ release from intracellular stores [53–55]. Addition of 2 μM Iono induced a similar $Ca^{2+}$ release in all groups examined, as determined by the quantification, which is represented as area under the curve (Fig. 3A,B; $P>0.05$). The other method tested was the addition of thapsigargin (TG), an inhibitor of the sarco/endoplasmic reticulum $Ca^{2+}$ ATPase [56], which also caused equivalent $[Ca^{2+}]_i$ responses in all groups (Fig. 3C,D; $P>0.05$), although the dynamics of the rises were different among the treatments. For example, time to peak was slower in $IP_3R1$-KD eggs than in controls eggs (Fig. 3E; $P<0.05$), and expression of wt-$IP_3R1$ exacerbated the difference (Fig. 3E; $P<0.001$), which was only partially improved by expression of IIIE-$IP_3R1$ (Fig. 3E; $P<0.001$). In total, the data show that $IP_3R1$ KD and expression of exogenous receptors do not alter the overall ER $Ca^{2+}$ releasable pool. The results also suggest that $IP_3R1$ is one of the channels that mediate $Ca^{2+}$ leak out of the ER, as its near complete elimination by KD, or following expression of exogenous receptors, which act in a dominant negative manner, greatly delayed the $Ca^{2+}$ leak induced by addition of TG.

## PLCζ cRNA induced $[Ca^{2+}]_i$ responses in $IP_3R1$-KD eggs expressing exogenous $IP_3R1$s

To compare the ability of wt-$IP_3R1$ and IIIE-$IP_3R1$ to support oscillations, we injected their cRNAs into $IP_3R1$-KD oocytes. Following *in vitro* maturation, $[Ca^{2+}]_i$ oscillations were induced by injection of 0.05 μg/μl PLCζ cRNA. In control eggs, injection of PLCζ cRNA induced $[Ca^{2+}]_i$ responses that started ~40 min after injection (Fig. 4A,B), occurred at mean intervals of 31.2±11.0 min (Fig. 4D), and terminated after ~5 spikes (Fig. 4A). In $IP_3R1$-KD eggs, the time to initiation and other $Ca^{2+}$ parameters were similar to those of control eggs (Fig. 4A–D; $P>0.05$), although these eggs only displayed 1 to 2 rises before ceasing (Fig. 4A). Expression of wt-$IP_3R1$ (Fig. 4A, KD+wt-$IP_3R1$) rescued the ability to initiate persistent oscillations, although the initiation of oscillations was delayed (Fig. 4B; $P<0.05$) and $[Ca^{2+}]_i$ rises occurred with lower frequency (Fig. 4D, $P<0.05$). Expression of IIIE-$IP_3R1$ in $IP_3R1$-KD eggs supported oscillations that greatly improved on those initiated in wt-$IP_3R1$ expressing eggs (Fig. 4A–E; $P<0.05$), although they still displayed delayed initiation and lower periodicity compared to control eggs (Fig. 4A, B, D; $P<0.05$). Remarkably, in IIIE-$IP_3R1$ expressing eggs, oscillations persisted well beyond those initiated in control eggs, sometimes in excess of 8 hrs (Fig. 4A; $P<0.05$), displayed greater amplitude (Fig. 4C; $P<0.05$) and their amplitude did not decline as oscillations persisted (Fig. 4A,E; $P<0.05$).

Together, the results suggest that modifications of $IP_3R1$ on M-phase kinase motifs enhance the ability of $IP_3R1$ receptor to support oscillations in mouse eggs.

## Phosphomimetic mutations at $S^{421}$, $S^{436}$ and $T^{799}$ enhance $IP_3R1$ sensitivity

We next examined the effect of the phosphomimetic mutations on $IP_3R1$ sensitivity. To accomplish this, cytosolic $IP_3$ concentrations were increased using caged $IP_3$ ($cIP_3$). Pulses of UV light of 0.25s and 0.75s duration, which released threshold and saturating concentrations respectively, were used sequentially to increase intracellular $IP_3$; the $[Ca^{2+}]_i$ responses induced by the photorelease of $IP_3$ were evaluated. Application of short pulses only caused reproducibly $[Ca^{2+}]_i$ responses in control eggs and in eggs expressing IIIE-$IP_3R1$ (Fig. 5A, left panel; 5B, $P<0.05$), although the duration of the rise was greater in the control group than in any of the other groups (Fig. 5D, $P<0.05$).

As expected, the longer UV pulse induced $[Ca^{2+}]_i$ responses in all eggs (Fig. 5A right panel; 5C, $P>0.05$), although the duration of the rise was greater in control eggs and in IIIE-$IP_3R1$-expressing eggs (Fig. 5E, $P>0.05$) and was lower in KD and wt-$IP_3R1$ eggs (Fig 4E, $P<0.05$), confirming the enhanced properties of IIIE-$IP_3R1$ channel over wt-$IP_3R1$.

## Endogenous and exogenous $IP_3R1$s display different stability

Agonist-induced degradation of $IP_3R1$ is one of the mechanisms that contribute to the termination of $[Ca^{2+}]_i$ responses in a variety of systems including eggs [34, 43, 57–60]. Because we observed that $[Ca^{2+}]_i$ oscillations induced by PLCζ cRNA injection in either wt-$IP_3R1$ or IIIE-$IP_3R1$ expressing eggs outlasted those induced in control eggs, we examined the impact of PLCζ cRNA-induced oscillations on the degradation of exogenous $IP_3R1$s using standard western blotting techniques.

Expression of exogenous, His-tagged wt-$IP_3R1$ or IIIE-$IP_3R1$ in eggs expressing the normal complement of $IP_3R1$ resulted in the appearance of two bands in the area corresponding to $IP_3R1$, which is similar to the pattern observed in Fig. 1B. We assume the upper band corresponds exclusively to the exogenous $IP_3R1$ and it will be designated hereafter as exogenous $IP_3R1$ (exo-$IP_3R1$), as the addition of 6×His tags on the C-terminus in the mutant IIIE-$IP_3R1$ are likely to delay migration (Fig. 6A). On the other hand, whereas the lower band is likely to contain mostly endogenous receptor, it cannot be discounted to also contain a portion of the exogenous receptors; we therefore designated this band as (endo-exo-$IP_3R1$). As expected, the levels of $IP_3R1$ in all groups remained unchanged following injection of buffer (Fig. 6A, left three lanes: 4 hr post MIB injection), which is consistent with the high stability of $IP_3R1$ in mouse eggs [34]. Nevertheless, injection of PLCζ cRNA induced degradation of most of $IP_3R1$ in control eggs, as only ~20% of $IP_3R1$ mass was left in these eggs. In comparison, in eggs expressing exogenous receptors, more than 60% of the total $IP_3R1$ signal mass was still present 4 hrs after the cRNA injection (Fig. 6B; $P<0.05$). Nevertheless, upon closer examination, we found most of the degradation happened in the lower band, which contains the majority of the endogenous receptors. As shown in Fig. 6C, while almost half of the signal corresponding to the endo-exo-$IP_3R1$ band disappeared 4 hr after PLCζ cRNA injection, ~80% of the signal of exo-$IP_3R1$ band remained. The same phenomenon was noticed in IIIE-$IP_3R1$ expressing eggs (Fig. 6C). Collectively, these data

suggest that in mouse eggs exogenous $IP_3R1$s are not degraded as efficiently as endogenous receptors, which may explain the longer persistence and steady amplitude of $[Ca^{2+}]_i$ oscillations in eggs expressing exogenous $IP_3R1$s.

## DISCUSSION

In the present study we examined the effects of phosphorylation by M-phase kinases, a type of modification that is thought to regulate the function of $IP_3R1$ in eggs. Constructs encoding for wt-$IP_3R1$ or an $IP_3R1$ with phosphomimetic mutations were generated followed by their expression and functional assessment in mouse eggs. Expression of exogenous receptors in the presence of endogenous receptors negatively impacted intracellular $Ca^{2+}$ signaling, i.e., caused dominant negative effects and restricted the ability of eggs to mount $[Ca^{2+}]_i$ oscillations. Therefore, to analyze the function of exogenous receptors, we first knocked-down endogenous receptors and subsequently expressed exogenous receptors. Our results show: 1) it is possible to down-regulate $IP_3R1$ while maintaining the organization of the ER largely intact as well as the levels of releasable $Ca^{2+}$ in the store; 2) expression of wt-$IP_3R1$ in $IP_3R1$-KD eggs achieved comparable distribution to that of the endogenous receptors and partly restored their $[Ca^{2+}]_i$ oscillatory ability, although did not rescue the normal ER cortical organization; 3) expression of $IP_3R1$s with phosphomimetic mutations corresponding to Cdk1 and ERK consensus sites enhanced $[Ca^{2+}]_i$ oscillations and increased $IP_3R1$ sensitivity over those supported by expression of wt-$IP_3R1$; 4) exogenous $IP_3R1$s seemed resistant to downregulation and supported longer oscillations and of higher amplitude. Collectively, this study establishes a novel system to evaluate the function of $IP_3R1$ receptors in mouse eggs and demonstrates that Cdk1- and MAPK-mediated phosphorylations are positive regulators of $IP_3R1$ function in mouse eggs.

### Expression of exogenous receptors compromises $[Ca^{2+}]_i$ responses in $IP_3R1$ intact eggs

To more specifically test the function of $IP_3R1$ in mouse eggs, we first expressed exogenous receptors in oocytes containing the full complement of endogenous $IP_3R1$. Surprisingly, exogenous receptors compromised the ability of mouse eggs to mount $[Ca^{2+}]_i$ oscillations, as PLCζ cRNA-initiated oscillations were delayed and showed less frequency than in control eggs. These results differ from those reported in somatic cells where the presence of additional receptors increased the overall receptor sensitivity of host cells [61–64]. In some of those reports, the somatic cell lines examined stably expressed the exogenous receptors, which is not the case in mouse oocytes, where expressed receptors can only be examined within 24 hr post-injection, as afterwards many cellular functions are compromised by aging of the cell. Therefore, due to the brief lifespan of fully-grown mouse oocytes, exogenous $IP_3R1$s do not undergo the post-translational modifications and/or interaction with other proteins and modulators that optimize their response and are therefore less capable of supporting oscillations [65–81]. There are several possible mechanisms whereby exogenous $IP_3R1$s can compromise the ability of mouse eggs to mount $[Ca^{2+}]_i$ oscillations. First, in somatic cells exogenous receptors form heterotetramers with endogenous receptors [15, 57]. If this were to happen in mouse oocytes, it would likely lower the sensitivity/conductivity of the heterotetramer receptor units. Alternatively, the presence of abundant homotetramers of exogenous receptors with inherently lower $IP_3$ affinity/sensitivity might act as an $IP_3$ sink,

increasing the threshold levels of $IP_3$ required to initiate oscillations thereby reducing the overall responsiveness of these eggs. Another formal possibility is that abnormal distribution of exogenous $IP_3R1$s could affect their ability to support $[Ca^{2+}]_i$ oscillations. Nevertheless, this does not appear to be the case, as exogenous receptors seemed to attain normal distribution when expressed in the presence (data not shown) or absence of endogenous receptors. Therefore, our studies show that expression of exogenous $IP_3R1$ in mouse eggs compromises the ability of the recipient eggs to mount $[Ca^{2+}]_i$ oscillations. Whether or not this is a unique phenomenon to oocytes and/or eggs is not known, as our studies are the first in mammalian eggs to express and evaluate the function of exogenous $IP_3R1$s. Exogenous receptors were expressed in *Xenopus* oocytes and eggs and their function were examined, although it is hard to draw comparisons because the longer time required to attain expression of the channel in these oocytes and the lack of oscillations in response to fertilization in *Xenopus* system [82, 83].

## Phosphomimetic mutations of M-phase kinase sites enhance $IP_3R1$ function

Consistent with its indispensable role underlying the events of egg activation and embryo development, the activity of $IP_3R1$ is enhanced during oocyte maturation [24, 28, 84, 85]. A purported mechanism that enhances $IP_3R1$ activity is phosphorylation [15, 17]. Others and we have found that cell cycle associated kinases, M-phase kinases, which are inherently involved in regulating the resumption of meiosis, phosphorylate $IP_3R1$ in eggs and this modification seems mostly to be associated with enhanced $Ca^{2+}$ releasing activity [27, 28, 33, 34, 86]. Nevertheless, in most of these studies, including reports in somatic cells, the evaluation of the impact of M-phase phosphorylations on receptor function was carried out in *in vitro* systems and/or using pharmacological inhibitors [33, 38, 42]. Therefore, to evaluate the effect of these modifications at the whole-cell level and also to bypass the confounding and detrimental influence of exogenous receptors on the endogenous $Ca^{2+}$-releasing machinery, we developed a system in which cRNAs for selected exogenous receptors are injected soon after the down-regulation of endogenous $IP_3R1$s. Using this approach, we showed that expression of wt-$IP_3R1$ restores the egg's ability to initiate persistent $[Ca^{2+}]_i$ oscillations, although the oscillations, which were initiated by injection of PLCζ cRNA were delayed and less frequent than in control eggs. These results confirm our findings that exogenous $IP_3R1$s in mouse eggs are not as efficient as endogenous receptors in supporting $[Ca^{2+}]_i$ oscillations. In spite of this limitation, we found that expression of IIIE-$IP_3R1$, which contained phosphomimetic mutations on three known M-phase motifs, reduced the lag time to initiation of oscillations and increased their frequency. These results suggest that M-phase mediated phosphorylations enhance the function of $IP_3R1$ in mouse eggs.

We extended these results by examining the sensitivity of exogenous $IP_3R1$s using $cIP_3$ technology. Our results show that whereas exogenous wt-$IP_3R1$s were much less responsive than endogenous $IP_3R1$s, the responses of IIIE-$IP_3R1$ expressing eggs were comparable to those of control eggs. It is worth noting that residues $S^{421}$ and $S^{436}$ lie in the $IP_3$ binding core domain of the receptor [87] and it is possible that IIIE-$IP_3R1$s have greater affinity for $IP_3$ than exogenous wt-$IP_3R1$s, as suggested by *in vitro* studies using somatic cells [38, 42]. We also found that expression of IIIE-$IP_3R1$ enhanced the duration of the $Ca^{2+}$ release

induced by the large $cIP_3$ pulse, which was greater than in wt-$IP_3R1$ expressing eggs and similar to control eggs. Several possibilities may explain these results, one of which is that phosphorylated $IP_3R1$s have greater channel open duration ($t_0$) and therefore greater conductivity, although more precise studies are needed to critically examine this possibility. We also cannot discount the prospect that IIIE-$IP_3R1$ expressing cells may modify $Ca^{2+}$ influx, as residue $T^{799}$ falls within the domain that is thought to interact with transient receptor potential channels (TRP), which are known mediators of $Ca^{2+}$ influx [87, 88]. Whereas recent evidence shows that TRPV3 channels are expressed in mouse oocytes/eggs [88], the role of these channels in $Ca^{2+}$ homeostasis in mouse eggs remains unknown. Another formal possibility is that the distribution/localization of IIIE-$IP_3R1$s is different than for exogenous WT receptors, which might underlie at least in part the greater responsiveness of IIIE-$IP_3R1$s. Studies should be conducted to rule out this possibility along with dose-titration experiments to ascertain that the expression levels of exogenous receptors are comparable. Lastly, we ruled out that the increased sensitivity of IIIE-$IP_3R1$s was due to higher $[Ca^{2+}]_{ER}$, as $[Ca^{2+}]_{ER}$ content was similar in all groups. Together, the enhanced $Ca^{2+}$-releasing properties observed in eggs IIIE-$IP_3R1$ vs. wt-$IP_3R1$ are consistent with the positive roles of M-phase phosphorylations on $IP_3R1$ function in eggs.

## Exogenously expressed $IP_3R1$s are resistant to down-regulation in mouse eggs

A striking feature of PLCζ cRNA-initiated $[Ca^{2+}]_i$ oscillations in eggs expressing wt-$IP_3R1$ or IIIE-$IP_3R1$ was the persistence of the responses, as in these eggs the oscillations outlasted those observed in control eggs. In mouse eggs, oscillations typically cease within 4 hr of injection/sperm entry [89, 90] and $[Ca^{2+}]_i$ rises show a protracted decline in amplitude. In KD+wt-$IP_3R1$ and KD+IIIE-$IP_3R1$ eggs, oscillations lasted in excess of 8 hr and unfolded without obvious decline in amplitude. Given that degradation of $IP_3R1$ contributes to the inactivation of sperm-initiated $[Ca^{2+}]_i$ oscillations [34, 43], we examined whether exogenous and endogenous $IP_3R1$s were equally degraded in these eggs. We found that whereas ~80% of endogenous $IP_3R1$ was degraded by 4 hr after injection of PLCζ cRNA, exogenous $IP_3R1$s seemed largely unchanged by the same time. This distinct downregulation of $IP_3R1$s in mouse eggs was surprising, as previous research in somatic cells has shown that exogenous $IP_3R1$s were similarly vulnerable to downregulation [61, 91]. Importantly, it was noticed that $IP_3R2$ and 3 were not equally susceptible to ubiquitylation, and that homotetramers of these isoforms were not targeted for degradation [91]. The reason for this discrepancy among $IP_3R$ isoforms was not explored, although it was postulated to be due to their cellular distribution, i.e. organization in clusters, which might protect receptors from degradation. It is unlikely that this occurs in eggs, as exogenous $IP_3R$s grossly attained similar distribution than endogenous receptors, although it is worthwhile noting that exogenous receptors were unable to rescue the cortical ER organization in $IP_3R1$-KD eggs. These results suggest that exogenous $IP_3R1$s are not able to associate with the same partners than endogenous $IP_3R1$s and that these degradation-resistant $IP_3R1$s might underlie the longer persistence and steady amplitude of PLCζ cRNA-initiated oscillations in wt-$IP_3R1$ and IIIE-$IP_3R1$ expressing eggs. The data also support the view that $IP_3R1$ function and degradation contribute to shape the pattern of oscillations during mammalian fertilization, as the oscillations in wt-$IP_3R1$ and IIIE-$IP_3R1$ expressing eggs were not only prolonged but showed steady amplitude.

Collectively our results show that M-phase kinase-mediated phosphorylations are important regulators of $IP_3R1$ function in mouse eggs. Further, our data suggest that exogenously expressed $IP_3R1$s, while capable of supporting $Ca^{2+}$ oscillations, are not as active as endogenous receptors. Understanding the mechanisms responsible for these differences may offer unique insights into the regulation of $IP_3R1$ function in mammalian oocytes and eggs, which could then be applied to increase the developmental competence of *in vitro* generated oocytes and embryos as well as to develop better parthenogenetic activation methods.

## MATERIAL AND METHODS

### Animal care and welfare

Animals used for gamete collections herein were handled following the National Research Council's Animal Care and Welfare Guidelines. These procedures were approved by the Institutional Animal Care and Use Committee at the University of Massachusetts.

### Egg collection and culture conditions

Superovulation was carried out as previously described (Gordo et al. 2002). CD-1 female mice, 6- to 8- week-old, were injected with 5 IU of pregnant mare serum gonadotropin (PMSG; Sigma, St Louis, MO; all chemicals were purchased from Sigma unless otherwise specified). Germinal vesicle (GV) oocytes were obtained from the ovaries 44 hr post PMSG in TL-HEPES supplemented with 5% heat-treated FCS and 100 μM 3-isobutyl-1-methylxanthine (IBMX). For maturation, GV oocytes were cultured for 12–14 hr in Chatot, Ziomek, and Bavister (CZB) medium [92] containing 0.1% PVA at 36.5°C and in a humidified atmosphere containing 5% $CO_2$. Normal matured eggs should extrude $1^{st}$ polar body.

### DNA Constructs and cRNA preparation

To construct the expression vector for wt-$IP_3R1$, the untranslated Kozak's sequence (GCCACC) and 5′-part (3.2kb, 1–3238) of $IP_3R1$ cDNA was amplified by PCR with primers 5′-GCAATACTCGAGGGCCACCATGTCTGACAAAATGTCG-3′ and 5′-CATTATGGGCCCCAGACACCAGGG-3′ (the underlined regions indicate XhoI and ApaI restriction endonuclease sites respectively) using mouse cerebellum $IP_3R1$ cDNA (a kind gift from Dr. K. Mikoshiba, Tokyo, Japan) in pcDNA-3.1(+) vector as a template. Likewise, the 3′ part (5.0kb, 3238–8247) of mouse $IP_3R1$ cDNA was amplified with primers 5′-GTGTCTGGGGCCCTGCAGCTCCTCTTTCGGCACTTCAGC-3′ and 5′-CTGCACACCGGTGGCCGGCTGCTGTGGGTTGACATTCATG-3′ (the underlined regions indicate ApaI and AgeI restriction endonuclease sites respectively). The two fragments were then sequentially subcloned into pcDNA6/myc-His B (Invitrogen, Carlsbad, CA) using the restriction endonuclease sites mentioned above.

To generate the constantly phosphorylated form of $IP_3R1$ (IIIE-$IP_3R1$), the 5′-part (3.2kb, 1–3238) and 3′ part (5.0kb, 3238–8247) of $IP_3R1$cDNA were firstly subcloned into vector pcDNA6/myc-His B separately using the same primers mentioned above. The two constructs were named $IP_3R1$(1–3238)-pcDNA6B and $IP_3R1$(3238–8247)-pcDNA6B. $IP_3R1$(1–3238)-pcDNA6B was then used as a template for the mutagenesis of both S421E

and S436E. $IP_3R1$(3238–8247)-pcDNA6B was used as a template for the mutagenesis of T799E. Mutagenesis was carried out using the QuikChange II XL Site-Directed Mutagenesis Kit (Stratagene, La Jolla, CA) according to the manufacture's protocol. Then the two mutated fragments were sequentially subcloned into pcDNA6/myc-His B (Invitrogen, Carlsbad, CA) using the same two restriction endonuclease sites mentioned above (ApaI and AgeI).

To construct the expression vector for ER-DsRed, the full-length sequence encoding for *Discosoma sp*. red fluorescent protein (DsRed2) with the ER targeting sequence of Calreticulin fused to the 5′ end and the ER retention sequence, KDEL fused to the 3′ end was a gift from Dr. Mohamed Trebak (The Centre for Cardiovascular Sciences, Albany Medical College, Albany, NY) to Dr. Wakai of the Fissore laboratory. This DsRed fused sequence was amplified by PCR and subcloned into the pcDNA6/myc-His B vector by Dr. Cheon of the Fissore lab.

After the sequences were confirmed (Genewiz, Cambridge, MA), the constructs were used for *in vitro* cRNA synthesis. Plasmids were linearized with AgeI and then transcribed from using the mMessage/mMachine T7 Kit (Ambion, Austin, TX). Poly A tail was added to the produced cRNA by Poly (A) Tailing kit (Ambion, Austin, TX) followed by purification using the MEGAclear Kit (Ambion, Austin, TX). cRNA was stored at −80°C in single-use aliquots.

## $[Ca^{2+}]_i$ imaging

$[Ca^{2+}]_i$ measurements were carried out as previously described, maximum of 20 eggs could be monitored together each time [93]. Eggs were loaded with 1.25 μM fura-2 AM (Molecular Probes, Eugene, OR) supplemented with 0.02% pluronic acid (Molecular Probes, Eugene, OR) for 20 minutes (min) at room temperature (RT). Eggs were then thoroughly washed and attached to glass-bottom dishes (MatTek Corp, Ashland, MA) in drops of FCS-free TL-HEPES under mineral oil, because eggs incline to stick to glass or plastic surface in the absence of protein source. $[Ca^{2+}]_i$ values were monitored using a Nikon Diaphot microscope fitted for fluorescence measurements. Eggs were simultaneously monitored using the software SimplePCI (C-Imaging System, Cranberry Township, PA), which controls a filter wheel rotating between excitation wavelengths of 340 and 380 nm illuminated by a 75 W Xenon arc lamp. Emitted light above 510 nm was collected by a cooled Photometrics SenSys CCD camera (Roper Scientific, Tucson, AZ) every 20 seconds (s) and used to calculate fluorescence ratios of 340/380 nm.

$[Ca^{2+}]_{ER}$ was estimated by assessing the magnitude of the $[Ca^{2+}]_i$ responses induced by addition of 10_μM thapsigargin (TG) (Thastrup et al. 1990) or 2 μM Ionomycin (Iono). Eggs were maintained in $Ca^{2+}$-free conditions, which were created by using TL-HEPES without adding $CaCl_2$ and supplemented with 1mM EGTA; TG or Iono was added to this media during $[Ca^{2+}]_i$ monitoring. $[Ca^{2+}]_i$ responses were then assessed by comparing the area-under-the-curve, which was calculated using the Prizm software (GraphPad Software, La Jolla, CA).

$IP_3$ induced $Ca^{2+}$ release was caused by caged$IP_3$ ($cIP_3$). Eggs were first injected with 0.5 mM $cIP_3$ (Molecular Probes) and then loaded with 1.25 μM Fluo-4 AM (Molecular Probes). $IP_3$ release was controlled by exposure to a 360 nm wavelength UV pulse. Fluo-4 excitation was accomplished with 488 nm wavelength and the emitted light collected as above; changes in $[Ca^{2+}]_i$ are expressed as $R = F/F_0$, where R is the fluorescence (F) normalized to the resting fluorescence ($F_0$). $F_0$ was calculated by averaging the first five fluorescent measurements for each egg prior to any treatment.

## Western blotting

Cell lysates from 40 or 20 cumulus-free eggs were prepared by adding 15μl of 2X sample buffer (SB) [94], as described previously (Jellerette et al. 2004). Samples were boiled for 3 min, loaded onto NuPAGE Novex 3–8% Tris-Acetate gels (Invitrogen, Carlsbad, CA), proteins were separated using electrophoresis for different durations (45 min for Fig. 1B; 60 min for Fig. 6A) and transferred onto nitrocellulose membranes (Micron Separations, Westboro, MA). To detect $IP_3R1$, the Rbt03 antibody (1/1000)[95] was used to detect $IP_3R1$. Anti-α-tubulin monoclonal antibody (1/1000, Sigma, St Louis, MO) was used to detect tubulin on the same membrane. The detection was accomplished by addition of a secondary HRP-conjugated goat anti-mouse antibody and chemiluminescence technology (NEN Life Science Products, Boston, MA). Blots were digitally recorded using a Kodak 440 Image Station (Rochester, NY). The same membranes were stripped at 50°C for 30 min (62.5 mM Tris, 2% SDS and 100 mM 2-beta mercaptoethanol) and were then used for detecting the overexpressed His with Anti-His monoclonal antibody (1/500, Invitrogen, Carlsbad, CA). The detection was accomplished by a HRP-labeled secondary antibody and the blots were digitally recorded using a Kodak 440 Image Station (Rochester, NY).

## Microinjection

Microinjection was performed as previously described [96]. In brief, eggs were microinjected under a Nikon Diaphot microscope (Nikon, Inc., Garden City, NY) using Narishige manipulators (Medical Systems Corp., Great Neck, NY). Reagents were loaded into glass micropipettes by aspiration and delivered by pneumatic pressure (PLI-100 picoinjector, Harvard Apparatus, Cambridge, MA). The injection volume was ~7–12 pl (1–3% of the total volume of the egg).

To prepare PLCζ cRNA for injection, the full-length sequence of mouse PLCζ (a kind gift from Dr K. Fukami, Tokyo University of Pharmacy and Life Science, Tokyo, Japan) within a pBluescript plasmid was in vitro transcribed using the T7 mMESSAGE mMACHINE Kit followed by poly A tailing (Ambion, Austin, TX), as reported previously [97]. Concentrated cRNA (2 μg/μl) was heated for 3 min at 85°C and diluted to 0.05 μg/μl in RNAase free water before microinjection. The cRNA of wt-$IP_3R1$, mutant forms $IP_3R1$ and ER-DsRed were heated for 3 min at 85 °C and then used for microinjection at its original concentration (2 μg/μl). 20 μM Adenophostin A (AdA) diluted in microinjection buffer (MIB) containing 75 mM KCl and 20 mM Hepes, pH 7.0 were delivered into the ooplasm by microinjection technique described above.

### Immunofluorescence

Following removal of the zona pellucida with acid tyrode's solution (pH 2.7) and after washes in 0.1% BSA-supplemented Dulbecco's PBS (DPBS-BSA), eggs were first fixed in 3.7% paraformaldehyde supplemented with 0.02% Triton X-100 and subsequently permeabilized with 0.1% Triton X-100 supplemented DPBS-BSA. Eggs were transferred into DPBS+5% normal goat serum (NGS-DPBS) for 2 hrs at 4 °C followed by overnight incubation at 4 °C with an anti-$IP_3R1$ primary antibody (CT1; 1/100; a generous gift of Dr R.J. Wojcikiewicz, SUNY Upstate Medical University) [58]. Following washing of the primary antibody, eggs were incubated with Alexa fluor 555-conjugated goat anti-rabbit IgG (Molecular Probes, Eugene, OR) for 1 hr at RT. Eggs were mounted using Vectashield Mounting Media (Vector Laboratories, Burlingame, CA, USA). Slides were examined at RT with a confocal laser-scanning microscope (510 META, Carl Zeiss Microimaging, Inc., Germany) using an Axiovert 2 microscope outfitted with a 63 × 1.4 NA oil immersion objective lens. Z-stack images were obtained from cortical to equatorial planes every 2 to 5 μm.

### ER membrane staining

$DiIC_{18}$, 1,1′-dioctadecyl-3,3,3′,3′-tetramethylindocarbocyanine perchlorate were obtained from Molecular Probes (Eugene, OR). A saturated solution of DiI in oil was made by mixing several crystals of DiI in 100 μl of soybean oil (Wesson oil, obtained from Stop&Shop, Amherst, MA). 30 min after the DiI solution was microinjected into eggs, eggs were captured using confocal microscope as described above. ER-DsRed cRNA was microinjected into GV oocytes as described above, then 14 hr after IVM MII eggs were imaged by confocal microscopy as described above. To count cortical clusters in ER-DsRed cRNA injected eggs, we randomly selected three eggs from each group in three independent experiments and counted the number of clusters of 1 μm in diameter or larger within a selected area (cortical area within yellow triangle in Fig. 2B) [45]. Image J was used to measure the diameters of the clusters [98].

### Electron microscopy

Changes of ER distribution in *in vitro* matured eggs including $IP_3R1$ KD or overexpression were monitored by transmission electron microscopy (TEM). TEM was performed as described earlier [99]. In brief, *in vitro* matured eggs were fixed with 2% glutaraldehyde and 4% paraformaldehyde in 0.05 M sodium cacodylate buffer (pH 7.2) for 2 hr. Fixed eggs were washed in 50mM cacodylate buffer (pH 7.2) and followed by post-fixing with 1% $OsO_4$ and 0.8% potassium ferricyanide for 60 min. Dehydration of fixed eggs was carried out by handing out eggs through 10 steps of increasing concentrations of acetone. Eggs were then embedded in epoxy resin and polymerized at 70°C for 2 hr. Eggs were sectioned by a Reichut-Jung Ultracut E ultramicrotone, and thin sections were double stained with uranyl acetate and lead citrate. Sections were examined under a Photometrics PXL camera integrated Tecnai 12 transmission electron microscope at an accelerating voltage of 80 kV (UMASS central microscope facility). For each treatment, at least three eggs were evaluated.

### Statistical analysis

Values from three or more experiments, performed on different batches of eggs, were used for evaluation of statistical significance. The Prism software (Graphpad Software) was used to draw graphs and perform the statistical comparisons using when appropriate Student's t-test or one-way ANOVA. Values are shown as means±S.E.M, and significant differences were considered at $p$ values <0.05.

## Acknowledgments

**Funding**

This work was supported by grant R01 HD051872 from the NIH to R.A.F.

## REFERENCES

1. Schultz RM, Kopf GS. Molecular basis of mammalian egg activation. Current topics in developmental biology. 1995; 30:21–62. [PubMed: 7555047]
2. Stricker SA. Comparative biology of calcium signaling during fertilization and egg activation in animals. Dev Biol. 1999; 211:157–176. [PubMed: 10395780]
3. Ducibella T, Huneau D, Angelichio E, Xu Z, Schultz RM, Kopf GS, Fissore R, Madoux S, Ozil JP. Egg-to-embryo transition is driven by differential responses to Ca(2+) oscillation number. Dev Biol. 2002; 250:280–291. [PubMed: 12376103]
4. Whitaker M, Swann K. Lighting the fuse at fertilization. Development. 1993; 117:1–12.
5. Epel D. The initiation of development at fertilization. Cell Differ. Dev. 1990; 29:1–12. [PubMed: 2154300]
6. Miyazaki S. Thirty years of calcium signals at fertilization. Seminars in Cell & Developmental Biology. 2006; 17:233–243. [PubMed: 16549376]
7. Ducibella T, Fissore R. The roles of Ca2+, downstream protein kinases, and oscillatory signaling in regulating fertilization and the activation of development. Dev Biol. 2008; 315:257–279. [PubMed: 18255053]
8. Miyazaki S, Hashimoto N, Yoshimoto Y, Kishimoto T, Igusa Y, Hiramoto Y. Temporal and spatial dynamics of the periodic increase in intracellular free calcium at fertilization of golden hamster eggs. Developmental Biology. 1986; 118:259–267. [PubMed: 3770302]
9. Saunders CM, Larman MG, Parrington J, Cox LJ, Royse J, Blayney LM, Swann K, Lai FA. PLC zeta: a sperm-specific trigger of Ca(2+) oscillations in eggs and embryo development. Development. 2002; 129:3533–3544. [PubMed: 12117804]
10. Fissore RA, Longo FJ, Anderson E, Parys JB, Ducibella T. Differential distribution of inositol trisphosphate receptor isoforms in mouse oocytes. Biol Reprod. 1999; 60:49–57. [PubMed: 9858485]
11. Parrington J, Brind S, De Smedt H, Gangeswaran R, Lai FA, Wojcikiewicz R, Carroll J. Expression of inositol 1,4,5-trisphosphate receptors in mouse oocytes and early embryos: the type I isoform is upregulated in oocytes and downregulated after fertilization. Dev Biol. 1998; 203:451–461. [PubMed: 9808793]
12. Miyazaki S, Yuzaki M, Nakada K, Shirakawa H, Nakanishi S, Nakade S, Mikoshiba K. Block of Ca2+ wave and Ca2+ oscillation by antibody to the inositol 1,4,5-trisphosphate receptor in fertilized hamster eggs. Science. 1992; 257:251–255. [PubMed: 1321497]
13. Berridge M, Lipp P, Bootman M. Calcium signalling. Current Biology : Cb. 1999; 9:R157–R159. [PubMed: 10074461]
14. Berridge MJ. Inositol trisphosphate and calcium signalling. Nature. 1993; 361:315–325. [PubMed: 8381210]
15. Patel S, Joseph SK, Thomas AP. Molecular properties of inositol 1,4,5-trisphosphate receptors. Cell Calcium. 1999; 25:247–264. [PubMed: 10378086]

16. Bosanac I, Michikawa T, Mikoshiba K, Ikura M. Structural insights into the regulatory mechanism of IP3 receptor. Biochimica et Biophysica Acta (BBA) -Molecular Cell Research. 2004; 1742:89–102. [PubMed: 15590059]
17. Patterson RL, Boehning D, Snyder SH. Inositol 1,4,5-trisphosphate receptors as signal integrators. Annual review of biochemistry. 2004; 73:437–465.
18. MacKrill JJ. Protein-protein interactions in intracellular Ca2+-release channel function. The Biochemical journal. 1999; 337(Pt 3):345–361. [PubMed: 9895277]
19. Parys JB, De Smedt H. Inositol 1,4,5-trisphosphate and its receptors. Adv Exp Med Biol. 2012; 740:255–279. [PubMed: 22453946]
20. Finch EA, Turner TJ, Goldin SM. Calcium as a coagonist of inositol 1,4,5-trisphosphate-induced calcium release. Science. 1991; 252:443–446. [PubMed: 2017683]
21. Iino M. Biphasic Ca2+ dependence of inositol 1,4,5-trisphosphate-induced Ca release in smooth muscle cells of the guinea pig taenia caeci. J Gen Physiol. 1990; 95:1103–1122. [PubMed: 2373998]
22. Bezprozvanny I, Watras J, Ehrlich BE. Bell-shaped calcium-response curves of Ins(1,4,5)P3- and calcium-gated channels from endoplasmic reticulum of cerebellum. Nature. 1991; 351:751–754. [PubMed: 1648178]
23. Parys JB, Sernett SW, DeLisle S, Snyder PM, Welsh MJ, Campbell KP. Isolation, characterization, and localization of the inositol 1,4,5-trisphosphate receptor protein in Xenopus laevis oocytes. J Biol Chem. 1992; 267:18776–18782. [PubMed: 1326534]
24. Fujiwara T, Nakada K, Shirakawa H, Miyazaki S. Development of Inositol Trisphosphate-Induced Calcium Release Mechanism during Maturation of Hamster Oocytes. Developmental Biology. 1993; 156:69–79. [PubMed: 8383620]
25. Kume S, Muto A, Aruga J, Nakagawa T, Michikawa T, Furuichi T, Nakade S, Okano H, Mikoshiba K. The Xenopus IP3 receptor: structure, function, and localization in oocytes and eggs. Cell. 1993; 73:555–570. [PubMed: 8387895]
26. Mehlmann LM, Kline D. Regulation of intracellular calcium in the mouse egg: calcium release in response to sperm or inositol trisphosphate is enhanced after meiotic maturation. Biology of Reproduction. 1994; 51:1088–1098. [PubMed: 7888488]
27. Sun L, Haun S, Jones RC, Edmondson RD, Machaca K. Kinase-dependent regulation of inositol 1,4,5-trisphosphate-dependent Ca2+ release during oocyte maturation. J Biol Chem. 2009; 284:20184–20196. [PubMed: 19473987]
28. Wakai T, Vanderheyden V, Yoon SY, Cheon B, Zhang N, Parys JB, Fissore RA. Regulation of inositol 1,4,5-trisphosphate receptor function during mouse oocyte maturation. Journal of cellular physiology. 2011
29. Vanderheyden V, Wakai T, Bultynck G, De Smedt H, Parys JB, Fissore RA. Regulation of inositol 1,4,5-trisphosphate receptor type 1 function during oocyte maturation by MPM-2 phosphorylation. Cell Calcium. 2009; 46:56–64. [PubMed: 19482353]
30. Bezprozvanny I. The inositol 1,4,5-trisphosphate receptors. Cell Calcium. 2005; 38:261–272. [PubMed: 16102823]
31. Vanderheyden V, Devogelaere B, Missiaen L, De Smedt H, Bultynck G, Parys JB. Regulation of inositol 1,4,5-trisphosphate-induced Ca2+ release by reversible phosphorylation and dephosphorylation. Biochim Biophys Acta. 2009; 1793:959–970. [PubMed: 19133301]
32. Kuang J, Ashorn C. At least two kinases phosphorylate the MPM-2 epitope during Xenopus oocyte maturation 10.1083/jcb.123.4.859. J. Cell Biol. 1993; 123:859–868. [PubMed: 7693720]
33. Lee B, Vermassen E, Yoon SY, Vanderheyden V, Ito J, Alfandari D, De Smedt H, Parys JB, Fissore RA. Phosphorylation of IP3R1 and the regulation of [Ca2+]i responses at fertilization: a role for the MAP kinase pathway. Development. 2006; 133:4355–4365. [PubMed: 17038520]
34. Jellerette T, He CL, Wu H, Parys JB, Fissore RA. Down-regulation of the inositol 1,4,5-trisphosphate receptor in mouse eggs following fertilization or parthenogenetic activation. Developmental Biology. 2000; 223:238–250. [PubMed: 10882513]
35. Solc P, Schultz RM, Motlik J. Prophase I arrest and progression to metaphase I in mouse oocytes: comparison of resumption of meiosis and recovery from G2-arrest in somatic cells. Mol Hum Reprod. 2010; 16:654–664. [PubMed: 20453035]

36. Nigg EA. The substrates of the cdc2 kinase. Semin Cell Biol. 1991; 2:261–270. [PubMed: 1842344]
37. Che S, Weil MM, Nelman-Gonzalez M, Ashorn CL, Kuang J. MPM-2 epitope sequence is not sufficient for recognition and phosphorylation by ME kinase-H. FEBS letters. 1997; 413:417–423. [PubMed: 9303547]
38. Malathi K, Kohyama S, Ho M, Soghoian D, Li X, Silane M, Berenstein A, Jayaraman T. Inositol 1,4,5-trisphosphate receptor (type 1) phosphorylation and modulation by Cdc2. J Cell Biochem. 2003; 90:1186–1196. [PubMed: 14635192]
39. Bai GR, Yang LH, Huang XY, Sun FZ. Inositol 1,4,5-trisphosphate receptor type 1 phosphorylation and regulation by extracellular signal-regulated kinase. Biochem Biophys Res Commun. 2006; 348:1319–1327. [PubMed: 16925983]
40. Yang LH, Bai GR, Huang XY, Sun FZ. ERK binds, phosphorylates InsP3 type 1 receptor and regulates intracellular calcium dynamics in DT40 cells. Biochemical and Biophysical Research Communications. 2006; 349:1339–1344. [PubMed: 16979595]
41. Matson S, Ducibella T. The MEK inhibitor, U0126, alters fertilization-induced [Ca2+]i oscillation parameters and secretion: differential effects associated with in vivo and in vitro meiotic maturation. Developmental Biology. 2007; 306:538–548. [PubMed: 17451670]
42. Malathi K, Li X, Krizanova O, Ondrias K, Sperber K, Ablamunits V, Jayaraman T. Cdc2/cyclin B1 interacts with and modulates inositol 1,4,5-trisphosphate receptor (type 1) functions. J Immunol. 2005; 175:6205–6210. [PubMed: 16237118]
43. Brind S, Swann K, Carroll J. Inositol 1,4,5-trisphosphate receptors are downregulated in mouse oocytes in response to sperm or adenophostin A but not to increases in intracellular Ca(2+) or egg activation. Developmental Biology. 2000; 223:251–265. [PubMed: 10882514]
44. Terasaki M, Jaffe LA. Organization of the sea urchin egg endoplasmic reticulum and its reorganization at fertilization. The Journal of Cell Biology. 1991; 114:929–940. [PubMed: 1874789]
45. Mehlmann LM, Terasaki M, Jaffe LA, Kline D. Reorganization of the endoplasmic reticulum during meiotic maturation of the mouse oocyte. Developmental Biology. 1995; 170:607–615. [PubMed: 7649387]
46. FitzHarris G, Marangos P, Carroll J. Changes in endoplasmic reticulum structure during mouse oocyte maturation are controlled by the cytoskeleton and cytoplasmic dynein. Dev Biol. 2007; 305:133–144. [PubMed: 17368610]
47. Wakai T, Zhang N, Vangheluwe P, Fissore RA. Regulation of endoplasmic reticulum Ca2+ oscillations in mammalian eggs. Journal of cell science. 2013
48. Zhang N, Fissore RA. Role of caspase-3 cleaved IP3 R1 on Ca(2+) homeostasis and developmental competence of mouse oocytes and eggs. J Cell Physiol. 2014; 229:1842–1854. [PubMed: 24692207]
49. Zhang N, Wakai T, Fissore RA. Caffeine alleviates the deterioration of Ca2+ release mechanisms and fragmentation of in vitro-aged mouse eggs. Molecular Reproduction and Development. 2011; 78:684–701. [PubMed: 22095868]
50. Takahashi T, Igarashi H, Kawagoe J, Amita M, Hara S, Kurachi H. Poor Embryo Development in Mouse Oocytes Aged In Vitro Is Associated with Impaired Calcium Homeostasis. Biol Reprod. 2009; 80:493–502. [PubMed: 19038861]
51. Kline D. Attributes and dynamics of the endoplasmic reticulum in mammalian eggs. Curr Top Dev Biol. 2000; 50:125–154. [PubMed: 10948453]
52. Jones KT, Carroll J, Whittingham DG. Ionomycin, thapsigargin, ryanodine, and sperm induced Ca2+ release increase during meiotic maturation of mouse oocytes. J Biol Chem. 1995; 270:6671–6677. [PubMed: 7896808]
53. Caridha D, Yourick D, Cabezas M, Wolf L, Hudson TH, Dow GS. Mefloquine-induced disruption of calcium homeostasis in mammalian cells is similar to that induced by ionomycin. Antimicrob Agents Chemother. 2008; 52:684–693. [PubMed: 17999964]
54. Shiina Y, Kaneda M, Matsuyama K, Tanaka K, Hiroi M, Doi K. Role of the extracellular Ca2+ on the intracellular Ca2+ changes in fertilized and activated mouse oocytes. Journal of reproduction and fertility. 1993; 97:143–150. [PubMed: 8464004]

55. Cuthbertson KS. Parthenogenetic activation of mouse oocytes in vitro with ethanol and benzyl alcohol. The Journal of experimental zoology. 1983; 226:311–314. [PubMed: 6864181]
56. Thastrup O, Cullen PJ, Drobak BK, Hanley MR, Dawson AP. Thapsigargin, a tumor promoter, discharges intracellular Ca2+ stores by specific inhibition of the endoplasmic reticulum Ca2(+)-ATPase. Proceedings of the National Academy of Sciences of the United States of America. 1990; 87:2466–2470. [PubMed: 2138778]
57. Zhu CC, Furuichi T, Mikoshiba K, Wojcikiewicz RJ. Inositol 1,4,5-trisphosphate receptor down-regulation is activated directly by inositol 1,4,5-trisphosphate binding. Studies with binding-defective mutant receptors. The Journal of biological chemistry. 1999; 274:3476–3484. [PubMed: 9920893]
58. Wojcikiewicz RJ, Furuichi T, Nakade S, Mikoshiba K, Nahorski SR. Muscarinic receptor activation down-regulates the type I inositol 1,4,5-trisphosphate receptor by accelerating its degradation. The Journal of Biological Chemistry. 1994; 269:7963–7969. [PubMed: 8132516]
59. Bokkala S, Joseph SK. Angiotensin II-induced down-regulation of inositol trisphosphate receptors in WB rat liver epithelial cells. Evidence for involvement of the proteasome pathway. The Journal of biological chemistry. 1997; 272:12454–12461. [PubMed: 9139693]
60. Sipma H, Deelman L, Smedt HD, Missiaen L, Parys JB, Vanlingen S, Henning RH, Casteels R. Agonist-induced down-regulation of type 1 and type 3 inositol 1,4,5-trisphosphate receptors in A7r5 and DDT1 MF-2 smooth muscle cells. Cell Calcium. 1998; 23:11–21. [PubMed: 9570006]
61. Zhu CC, Furuichi T, Mikoshiba K, Wojcikiewicz RJ. Inositol 1,4,5-trisphosphate receptor down-regulation is activated directly by inositol 1,4,5-trisphosphate binding. Studies with binding-defective mutant receptors. J Biol Chem. 1999; 274:3476–3484. [PubMed: 9920893]
62. Miyawaki A, Furuichi T, Maeda N, Mikoshiba K. Expressed cerebellar-type inositol 1,4,5-trisphosphate receptor, P400, has calcium release activity in a fibroblast L cell line. Neuron. 1990; 5:11–18. [PubMed: 2164403]
63. Mackrill JJ, Wilcox RA, Miyawaki A, Mikoshiba K, Nahorski SR, Challiss RA. Stable overexpression of the type-1 inositol 1,4,5-trisphosphate receptor in L fibroblasts: subcellular distribution and functional consequences. Biochem J. 1996; 318(Pt 3):871–878. [PubMed: 8836131]
64. Blondel O, Bell GI, Moody M, Miller RJ, Gibbons SJ. Creation of an inositol 1,4,5-trisphosphate-sensitive Ca2+ store in secretory granules of insulin-producing cells. J Biol Chem. 1994; 269:27167–27170. [PubMed: 7961623]
65. Cameron AM, Steiner JP, Roskams AJ, Ali SM, Ronnett GV, Snyder SH. Calcineurin associated with the inositol 1,4,5-trisphosphate receptor-FKBP12 complex modulates Ca2+ flux. Cell. 1995; 83:463–472. [PubMed: 8521476]
66. Cameron AM, Steiner JP, Sabatini DM, Kaplin AI, Walensky LD, Snyder SH. Immunophilin FK506 binding protein associated with inositol 1,4,5-trisphosphate receptor modulates calcium flux. Proceedings of the National Academy of Sciences of the United States of America. 1995; 92:1784–1788. [PubMed: 7533300]
67. Kasri NN, Holmes AM, Bultynck G, Parys JB, Bootman MD, Rietdorf K, Missiaen L, McDonald F, Smedt HD, Conway SJ, Holmes AB, Berridge MJ, Roderick HL. Regulation of InsP(3) receptor activity by neuronal Ca(2+)-binding proteins. The Embo Journal. 2004; 23:312–321. [PubMed: 14685260]
68. Mignery GA, Johnston PA, Sudhof TC. Mechanism of Ca2+ inhibition of inositol 1,4,5-trisphosphate (InsP3) binding to the cerebellar InsP3 receptor. The Journal of Biological Chemistry. 1992; 267:7450–7455. [PubMed: 1313802]
69. Sienaert I, De Smedt H, Parys JB, Missiaen L, Vanlingen S, Sipma H, Casteels R. Characterization of a cytosolic and a luminal Ca2+ binding site in the type I inositol 1,4,5-trisphosphate receptor. The Journal of Biological Chemistry. 1996; 271:27005–27012. [PubMed: 8900188]
70. Cui J, Matkovich SJ, deSouza N, Li S, Rosemblit N, Marks AR. Regulation of the Type 1 Inositol 1,4,5-Trisphosphate Receptor by Phosphorylation at Tyrosine 353. J. Biol. Chem. 2004; 279:16311–16316. [PubMed: 14761954]

71. Zhang S, Malmersjo S, Li J, Ando H, Aizman O, Uhlen P, Mikoshiba K, Aperia A. Distinct role of the N-terminal tail of the Na,K-ATPase catalytic subunit as a signal transducer. J Biol Chem. 2006; 281:21954–21962. [PubMed: 16723354]
72. Miyakawa-Naito A, Uhlen P, Lal M, Aizman O, Mikoshiba K, Brismar H, Zelenin S, Aperia A. Cell signaling microdomain with Na,K-ATPase and inositol 1,4,5-trisphosphate receptor generates calcium oscillations. The Journal of Biological Chemistry. 2003; 278:50355–50361. [PubMed: 12947118]
73. Ferris CD, Huganir RL, Bredt DS, Cameron AM, Snyder SH. Inositol trisphosphate receptor: phosphorylation by protein kinase C and calcium calmodulin-dependent protein kinases in reconstituted lipid vesicles. Proceedings of the National Academy of Sciences of the United States of America. 1991; 88:2232–2235. [PubMed: 1848697]
74. Vermassen E, Fissore RA, Nadif Kasri N, Vanderheyden V, Callewaert G, Missiaen L, Parys JB, De Smedt H. Regulation of the phosphorylation of the inositol 1,4,5-trisphosphate receptor by protein kinase C. Biochem Biophys Res Commun. 2004; 319:888–893. [PubMed: 15184066]
75. Jayaraman T, Ondrias K, Ondriasova E, Marks AR. Regulation of the inositol 1,4,5-trisphosphate receptor by tyrosine phosphorylation. Science. 1996; 272:1492–1494. [PubMed: 8633244]
76. Yokoyama K, Su Ih IH, Tezuka T, Yasuda T, Mikoshiba K, Tarakhovsky A, Yamamoto T. BANK regulates BCR-induced calcium mobilization by promoting tyrosine phosphorylation of IP(3) receptor. The Embo Journal. 2002; 21:83–92. [PubMed: 11782428]
77. Singleton PA, Bourguignon LY. CD44v10 interaction with Rho-kinase (ROK) activates inositol 1,4,5-triphosphate (IP3) receptor-mediated Ca2+ signaling during hyaluronan (HA)-induced endothelial cell migration. Cell Motil Cytoskeleton. 2002; 53:293–316. [PubMed: 12378540]
78. Khan MT, Wagner L 2nd, Yule DI, Bhanumathy C, Joseph SK. Akt kinase phosphorylation of inositol 1,4,5-trisphosphate receptors. The Journal of Biological Chemistry. 2006; 281:3731–3737. [PubMed: 16332683]
79. DeSouza N, Reiken S, Ondrias K, Yang YM, Matkovich S, Marks AR. Protein kinase A and two phosphatases are components of the inositol 1,4,5- trisphosphate receptor macromolecular signaling complex. The Journal of Biological Chemistry. 2002; 277:39397–39400. [PubMed: 12167631]
80. Vanlingen S, Sipma H, Missiaen L, De Smedt H, De Smet P, Casteels R, Parys JB. Modulation of type 1, 2 and 3 inositol 1,4,5-trisphosphate receptors by cyclic ADP-ribose and thimerosal. Cell Calcium. 1999; 25:107–114. [PubMed: 10326677]
81. Bandyopadhyay BC, Ong HL, Lockwich TP, Liu X, Paria BC, Singh BB, Ambudkar IS. TRPC3 controls agonist-stimulated intracellular Ca2+ release by mediating the interaction between inositol 1,4,5-trisphosphate receptor and RACK1. J Biol Chem. 2008; 283:32821–32830. [PubMed: 18755685]
82. Miyawaki A, Matheson JM, Sayers LG, Muto A, Michikawa T, Furuichi T, Mikoshiba K. Expression of green fluorescent protein and inositol 1,4,5-triphosphate receptor in Xenopus laevis oocytes. Methods Enzymol. 1999; 302:225–233. [PubMed: 12876775]
83. Sun L, Yu F, Ullah A, Hubrack S, Daalis A, Jung P, Machaca K. Endoplasmic reticulum remodeling tunes IP(3)-dependent Ca(2)+ release sensitivity. PLoS One. 2011; 6:e27928. [PubMed: 22140486]
84. Xu Z, Kopf G, Schultz R. Involvement of inositol 1,4,5-trisphosphate-mediated Ca2+ release in early and late events of mouse egg activation, Development (Cambridge. England). 1994; 120:1851–1859.
85. Xu Z, Williams CJ, Kopf GS, Schultz RM. Maturation-associated increase in IP3 receptor type 1: role in conferring increased IP3 sensitivity and Ca2+ oscillatory behavior in mouse eggs. Dev Biol. 2003; 254:163–171. [PubMed: 12591238]
86. Ito J, Yoon SY, Lee B, Vanderheyden V, Vermassen E, Wojcikiewicz R, Alfandari D, De Smedt H, Parys JB, Fissore RA. Inositol 1,4,5-trisphosphate receptor 1, a widespread Ca2+ channel, is a novel substrate of polo-like kinase 1 in eggs. Dev Biol. 2008; 320:402–413. [PubMed: 18621368]
87. Foskett JK, White C, Cheung KH, Mak DO. Inositol trisphosphate receptor Ca2+ release channels. Physiol Rev. 2007; 87:593–658. [PubMed: 17429043]

88. Carvacho I, Lee HC, Fissore RA, Clapham DE. TRPV3 channels mediate strontium-induced mouse-egg activation. Cell reports. 2013; 5:1375–1386. [PubMed: 24316078]

89. Deguchi R, Shirakawa H, Oda S, Mohri T, Miyazaki S. Spatiotemporal analysis of Ca(2+) waves in relation to the sperm entry site and animal-vegetal axis during Ca(2+) oscillations in fertilized mouse eggs. Developmental Biology. 2000; 218:299–313. [PubMed: 10656771]

90. Ito M, Shikano T, Oda S, Horiguchi T, Tanimoto S, Awaji T, Mitani H, Miyazaki S. Difference in Ca2+ oscillation-inducing activity and nuclear translocation ability of PLCZ1, an egg-activating sperm factor candidate, between mouse, rat, human, and medaka fish. Biology of Reproduction. 2008; 78:1081–1090. [PubMed: 18322275]

91. Oberdorf J, Webster JM, Zhu CC, Luo SG, Wojcikiewicz RJ. Down-regulation of types I, II and III inositol 1,4,5-trisphosphate receptors is mediated by the ubiquitin/proteasome pathway. Biochem J. 1999; 339(Pt 2):453–461. [PubMed: 10191279]

92. Chatot CL, Ziomek CA, Bavister BD, Lewis JL, Torres I. An improved culture medium supports development of random-bred 1-cell mouse embryos in vitro. Journal of reproduction and fertility. 1989; 86:679–688. [PubMed: 2760894]

93. Kurokawa M, Fissore RA. ICSI-generated mouse zygotes exhibit altered calcium oscillations, inositol 1,4,5-trisphosphate receptor-1 down-regulation, and embryo development. Mol Hum Reprod. 2003; 9:523–533. [PubMed: 12900511]

94. Laemmli UK. Cleavage of structural proteins during the assembly of the head of bacteriophage T4. Nature. 1970; 227:680–685. [PubMed: 5432063]

95. Parys JB, de Smedt H, Missiaen L, Bootman MD, Sienaert I, Casteels R. Rat basophilic leukemia cells as model system for inositol 1,4,5-trisphosphate receptor IV, a receptor of the type II family: functional comparison and immunological detection. Cell Calcium. 1995; 17:239–249. [PubMed: 7664312]

96. Gordo AC, Rodrigues P, Kurokawa M, Jellerette T, Exley GE, Warner C, Fissore R. Intracellular calcium oscillations signal apoptosis rather than activation in in vitro aged mouse eggs. Biol Reprod. 2002; 66:1828–1837. [PubMed: 12021069]

97. Kurokawa M, Sato K, Smyth J, Wu H, Fukami K, Takenawa T, Fissore RA. Evidence that activation of Src family kinase is not required for fertilization-associated [Ca2+]i oscillations in mouse eggs. 2004; 127:441–454.

98. Schneider CA, Rasband WS, Eliceiri KW. NIH Image to ImageJ: 25 years of image analysis. Nat Methods. 2012; 9:671–675. [PubMed: 22930834]

99. Knott JG, Kurokawa M, Fissore RA. Release of the Ca(2+) oscillation-inducing sperm factor during mouse fertilization. Dev Biol. 2003; 260:536–547. [PubMed: 12921751]

## Highlights

- Downregulation of $IP_3R1$ inhibits persistent $Ca^{2+}$ oscillations in mouse eggs
- Expression of wild type $IP_3R1$ rescues ability to mount persistent $Ca^{2+}$ oscillations
- $IP_3R1$s with phosphomimetic mutations show higher function and oscillations
- Exogenous $IP_3R1$ s are resistant to downregulation, which enhance oscillations

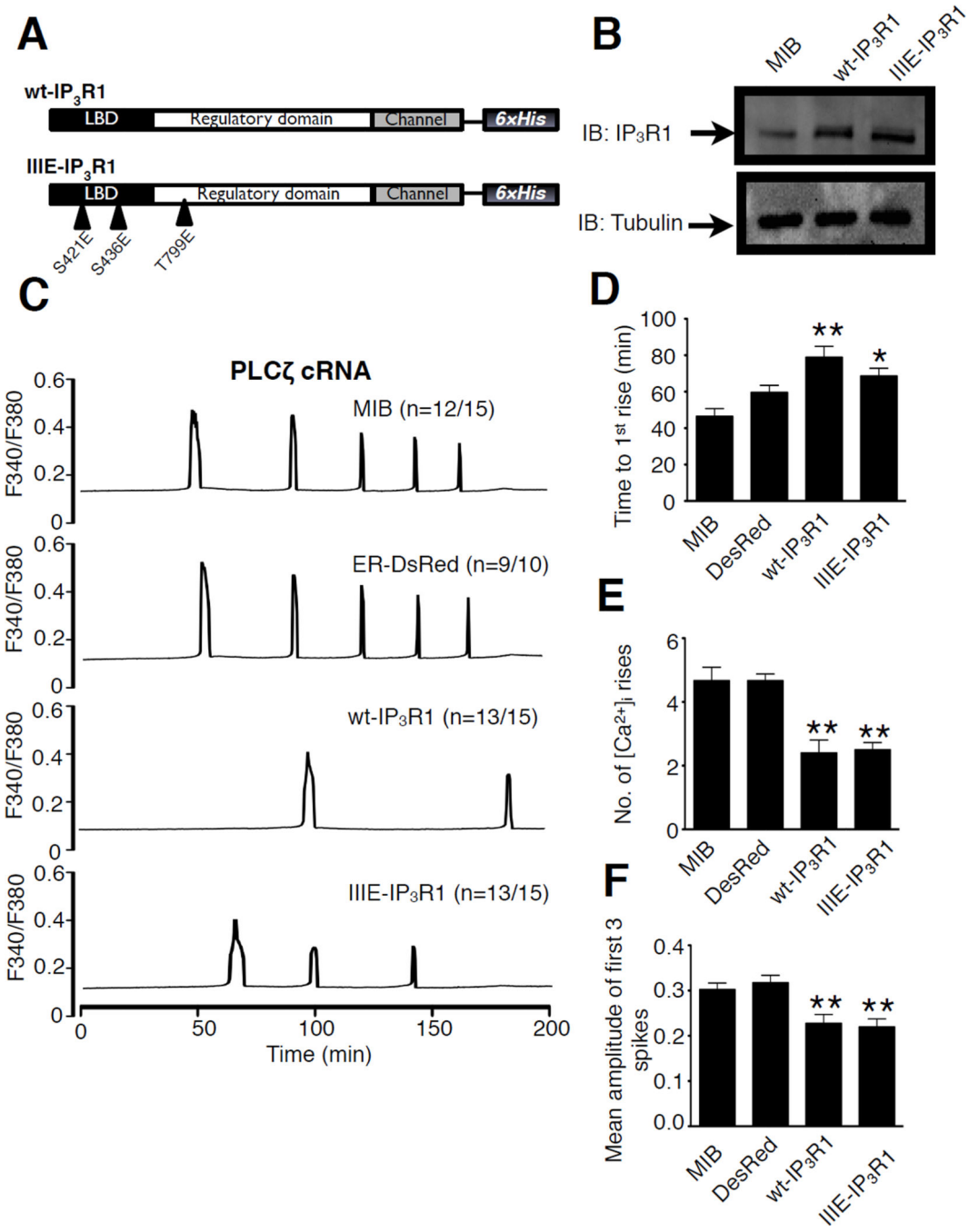


**Figure 1. Expression of different IP$_3$R1 constructs in mouse oocytes and dominant negative effects of expressed IP$_3$R1 on endogenous receptors**

(A) Molecular structure of IP$_3$R1 comprising three functionally distinct domains; wild type IP$_3$R1 (wt-IP$_3$R1) and phosphomimetic mutated IP$_3$R1 (IIIE-IP$_3$R1) are depicted. LBD: ligand-binding domain. The C-terminal 6xHis tag is indicated as well as the mutated phosphorylation sites (IIIE-IP$_3$R1). (B) Immunoblotting of 20-cell lysates from GV oocytes 4–6 hr after injection of microinjection buffer (MIB), wt-IP$_3$R1 or IIIE-IP$_3$R1 cRNAs, probed with Rbt03 antibody and anti–α-tubulin antibody. (C) Changes in $[Ca^{2+}]_i$ induced by injection of PLCζ cRNA (0.05μg/μl) in IVM eggs injected with MIB, or expressing ER-

DsRed, wt-$IP_3R1$ or IIIE-$IP_3R1$. (D-F) Statistical comparison of the different parameters of $Ca^{2+}$ oscillatory responses in eggs injected with MIB, or expressing ER-DsRed, wt-$IP_3R1$ or IIIE-$IP_3R1$, including time to $1^{st}$ rise (D), number of spikes (E), and mean amplitude of the first 3 spikes (F). Bars with one asterisk are different from those without them with $P<0.05$. Bars with two asterisks are different from those without them with $P<0.01$.

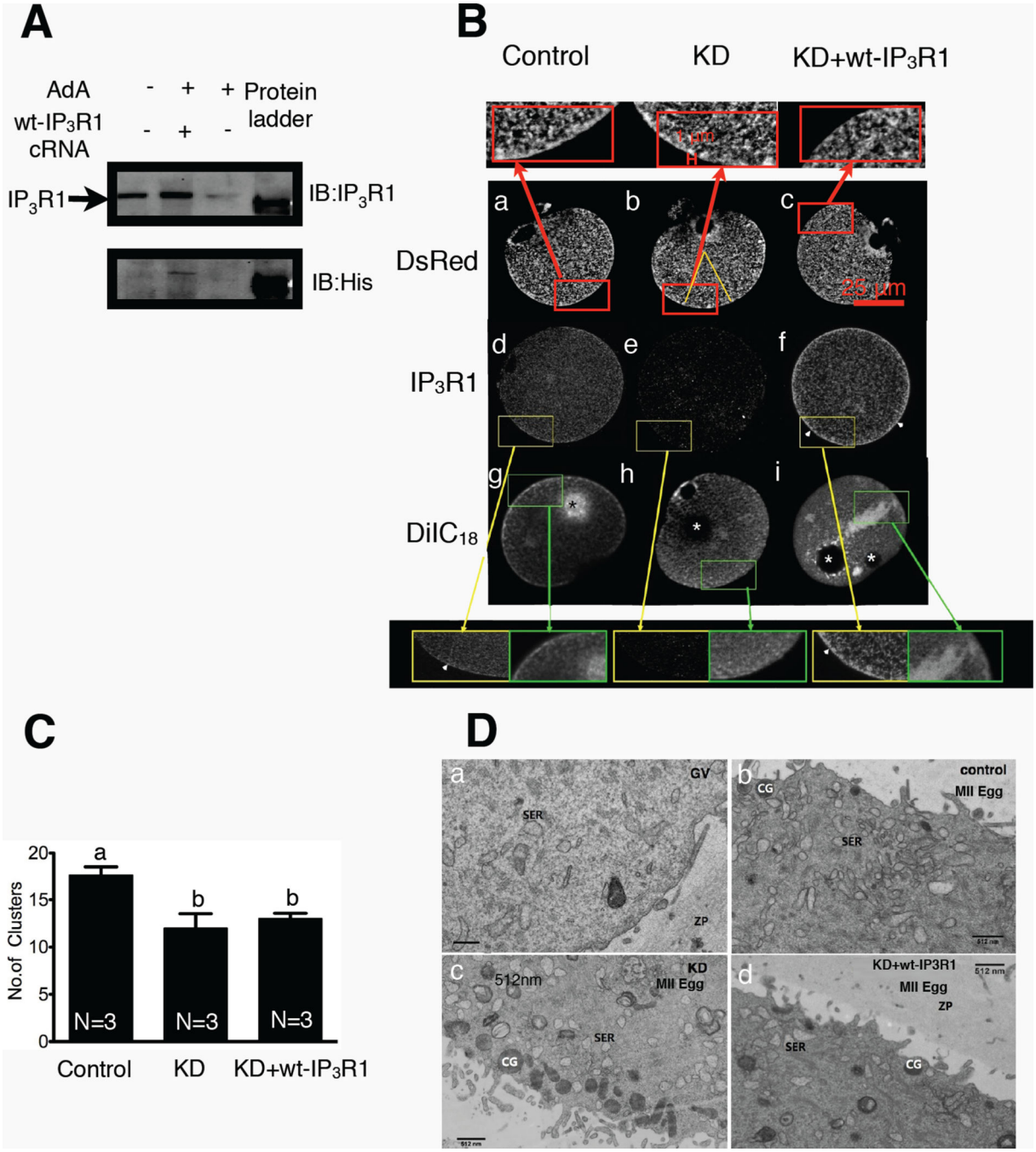


**Figure 2. Knockdown and expression of $IP_3R1$ in mouse oocytes and their effects on the architecture of the ER**

(A) Immunoblotting of 40-cell lysates from IVM control eggs (1st lane), $IP_3R1$ KD plus wt-$IP_3R1$ expressing cells (2nd lane) and $IP_3R1$ KD eggs (3rd lane); probed with Rbt03 antibody and anti-His antibody. (B) ER and $IP_3R1$ staining imaged by confocal microscope. DsRed panel: ER membrane organization as reported by expressed ER-DsRed fluorescence in control IVM eggs (a), $IP_3R1$ KD eggs (b), and KD+wt-$IP_3R1$ overexpression eggs (c). $IP_3R1$ panel: Immunostaining of $IP_3R1$ distribution in the various groups of mouse oocytes as described before (d,e,f). $DiIC_{18}$ panel: ER membrane staining with $DiIC_{18}$ in the same

groups of mouse oocytes as described before (g,h,i). The areas denoted by a rectangle are shown in a magnified version above or below the images. Arrowheads in d and f denote cortical accumulation of $IP_3R1$s (clusters). The white asterisks in h and I denote the locations of soybean oil droplets and the black asterisk in g denotes excessive dye accumulation, possibly caused by prolonged incubation prior to observation. (C) Bar graph displaying a comparison of numbers of ER cortical clusters in ER-DsRed cRNA injected eggs. Clusters of ≥1 μm in diameter were counted within a selected area denoted by a yellow triangle ($P<0.05$). (D) Transmission electron micrographs of the cortex of GV oocytes (a), IVM eggs (b), $IP_3R1$ KD eggs (c) and KD + wt-$IP_3R1$ eggs (d).

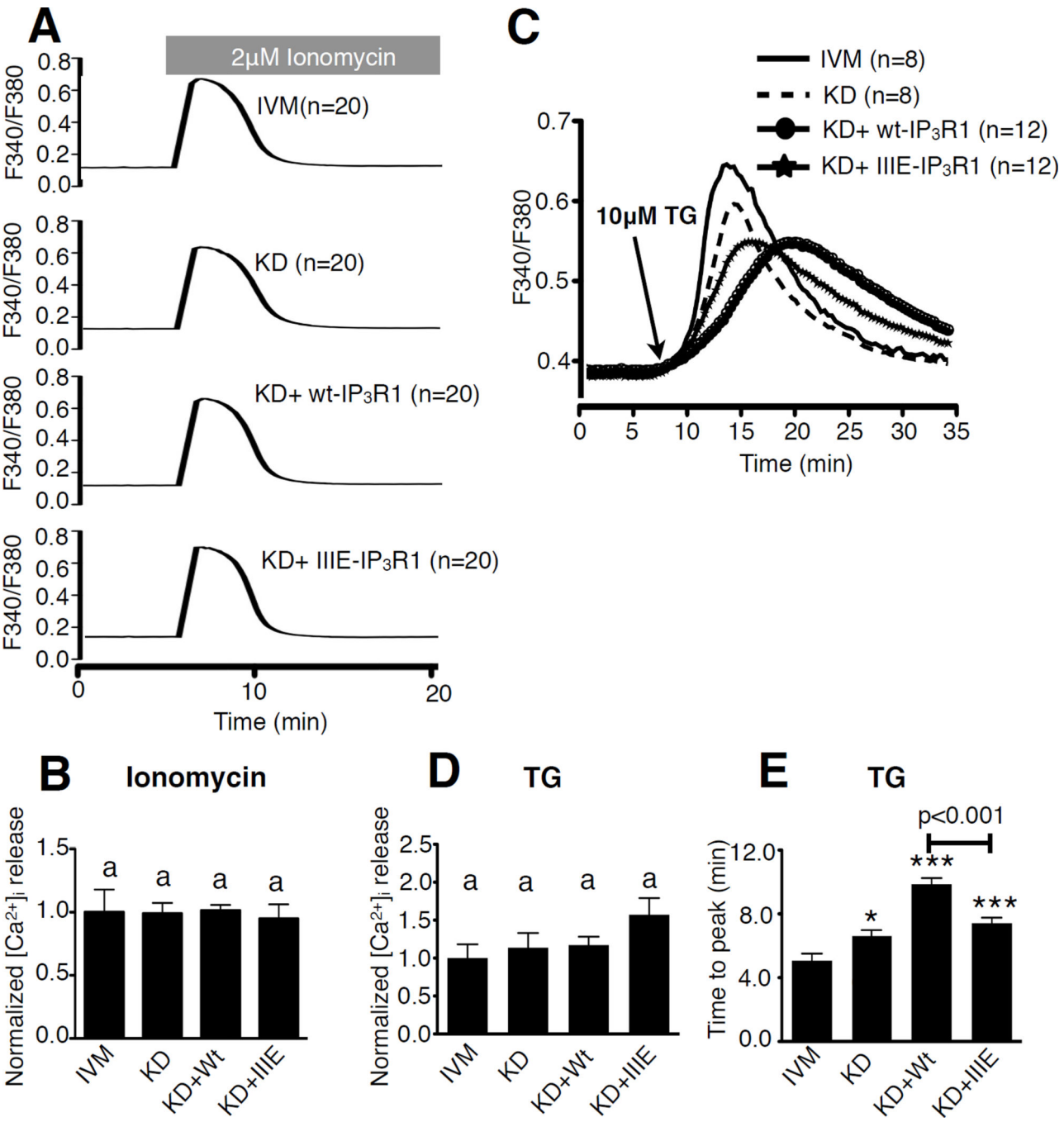


**Figure 3. Knockdown and expression of $IP_3R1$ do not affect $[Ca^{2+}]_{ER}$ in mouse oocytes**

(A) Representative $[Ca^{2+}]_i$ profiles of $Ca^{2+}$ release from the ER induced by addition of 2 μM Ionomycin (Iono) in IVM, KD, KD+wt-$IP_3R1$ and KD+IIIE-$IP_3R1$ eggs. (B) Area under the curve for Iono-induced $Ca^{2+}$ release was calculated; IVM was chosen as 100% and values for the other groups were presented relative to 100%. (C) Representative $[Ca^{2+}]_i$ profiles of $Ca^{2+}$ release from the ER induced by addition of 10 μM thapsigargin (TG) in IVM, KD, KD +wt-$IP_3R1$ and KD+IIIE-$IP_3R1$ eggs. (D) Area under the curve for TG-induced $Ca^{2+}$ release was calculated; IVM was chosen as 100% and values for the other groups were presented

relative to 100%. Bars with the same superscripts represent treatments that are not significantly different (P>0.05). (E) Statistical comparison of the time the $[Ca^{2+}]_i$ responses in eggs of each group took to reach the peak in Fig 3C. Bars with asterisks represent treatments that are different from IVM group (*P<0.05 and *** P<0.001). The KD+Wt group is also significantly different from KD+IIIE group (P<0.001).

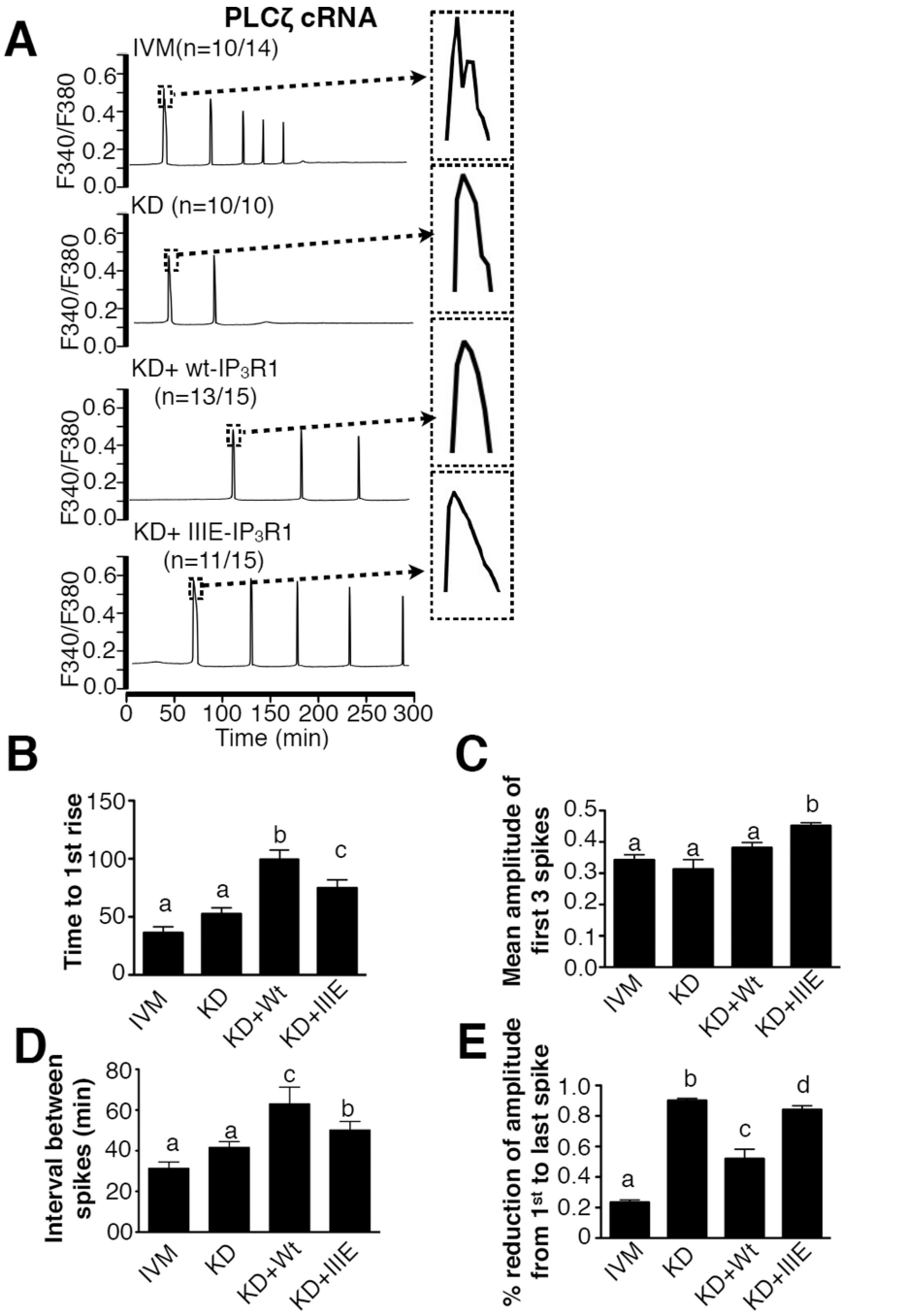


**Figure 4. CDK- and ERK-related phosphorylations on $IP_3R1$ enhance $Ca^{2+}$ oscillations in mouse oocytes**

(A) Changes in $[Ca^{2+}]_i$ induced by injection of PLCζ cRNA (0.05 μg/μl) in IVM, KD, KD +wt-$IP_3R1$ and KD+IIIE-$IP_3R1$ eggs. (B-D) Statistical comparison of parameters of $Ca^{2+}$ oscillatory responses in the IVM, KD, KD+wt-$IP_3R1$ and KD+IIIE-$IP_3R1$ eggs, including time to 1st rise (B), mean amplitude of the first 3 spikes (C), interval between spikes (D) and the % reduction of amplitude from 1st to last spike (E). Bars with different superscripts represent treatments that are significantly different ($P<0.05$).

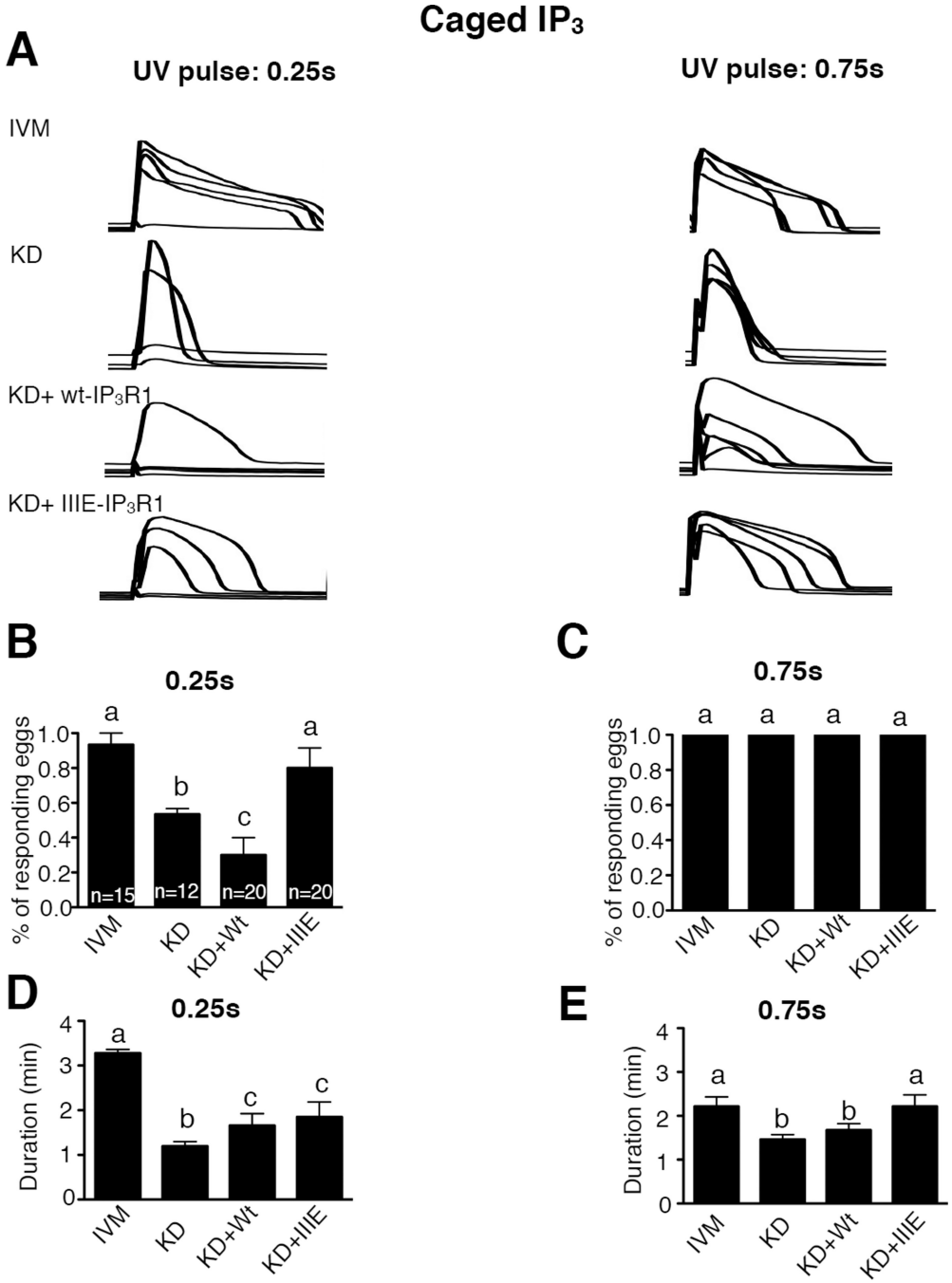


**Figure 5. CDK- and ERK-related phosphorylations on $IP_3R1$ enhance the sensitivity of $IP_3R1$ in mouse oocytes**

(A) Changes in $[Ca^{2+}]_i$ induced by photolysis of $cIP_3$ in IVM, KD, KD+wt-$IP_3R1$ and KD +IIIE-$IP_3R1$ mouse eggs. Two UV pulses with different duration (0.25s and 0.75s) were conducted sequentially and noted in each of the panels. The number of responding eggs expressed in % (B,C) and the duration of the $Ca^{2+}$ release (D,E) caused by a 0.25s and 0.75s UV pulse were compared among the different treatments mentioned above. Bars with different superscripts represent treatments that are significantly different ($P<0.05$).

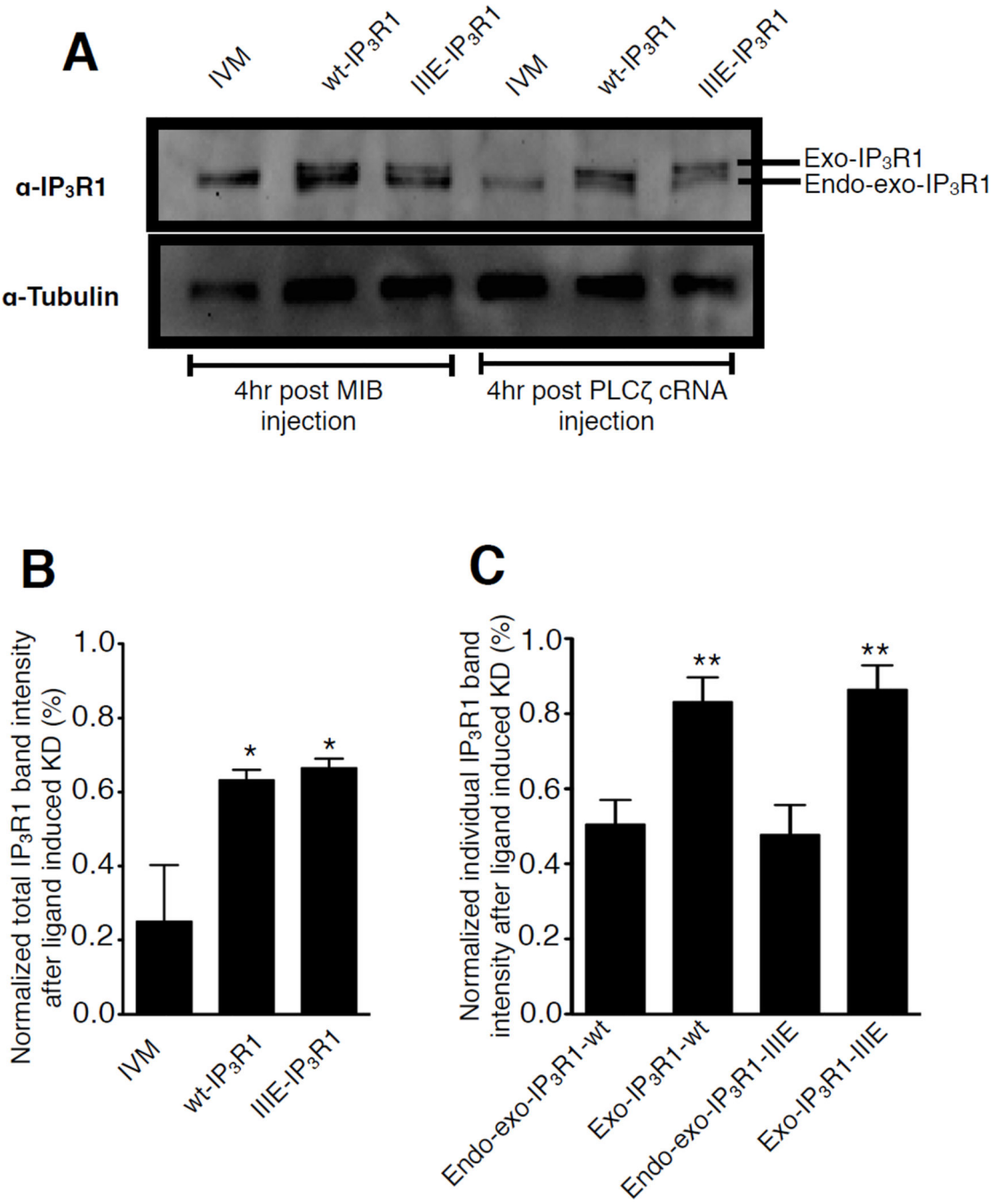


**Figure 6. Differential PLCζ-induced degradation rate of endogenous and exogenous IP$_3$R1s in mouse oocytes**

(A) Immunoblotting of egg lysates from IVM eggs, wt-IP$_3$R1 and IIIE-IP$_3$R1 expressing eggs 4hr after MIB or PLCζ cRNA injection, probed with the Rbt03 antibody and anti–α-tubulin antibody. (B) Intensity of the total IP$_3$R1 signal including the upper (Exo-IP$_3$R1) and lower bands (Endo-exo-IP$_3$R1) from panel A 4 hr after PLCζ cRNA injection was calculated. (C) Intensity of the Exo-IP$_3$R1 and Endo-exo-IP$_3$R1 bands was calculated separately in the groups of 6A. In both panels B and C, the amount present in IVM, wt-IP$_3$R1 and IIIE-IP$_3$R1 eggs after injection with MIB was chosen as control and set at 100%;

the band intensities observed in IVM, wt-$IP_3R1$ and IIIE-$IP_3R1$ eggs injected with PLCζ cRNA were presented relative to the control condition.